Universidad de La Laguna

Trabajo de Fin de Máster

QUANTUM LANGEVIN EQUATIONS: energy transport properties in harmonic systems

Tanausú Hernández Yanes

Supervised by
Dr. Antonia Ruiz García and Dr. José Pascual Palao González

Trabajo de fin de máster
Master universitario en Astrofísica
Escuela de doctorado y estudios de posgrado
Departamento de Física

September 10, 2019

Abstract

This work serves as an introduction into open quantum systems by means of a system plus reservoir approach which allows us to obtain analytic results for the covariance matrix at the steady state. The reservoir model employed will be the Caldeira-Legget bath model, a popular approach based on an environment composed of a large amount of harmonic oscillators, and we will limit the study to the steady state of the system in order to obtain analytical results. The elements of the covariance matrix allows to study properties of the system through different scenarios where we obtain temperature profiles for a chain of oscillators under the absence of an intermediate bath or the heat currents under different regimes. In particular, we observe the effects of a defect in the coupling between oscillators of the chain and confirm the heat transport through an intermediate bath without the need of coupling between the oscillators of the same bath.

Contents

Chapter 1

Introduction

When a large and complex quantum system is studied it is convenient to disregard the many or even infinite constituents of it in order to employ them as a means to obtain simple and few dynamical variables, achieving a global description. Thus, the study of open quantum systems becomes highly relevant when we are interested in the physical properties of the particular components of a larger system. There are multiple methods to obtain this description, such as the functional integral approach, state vectors in Hilbert space or system plus reservoir methods [1]. In the following chapters we will delve in the latter method, specifically in the harmonic oscillator bath approach with linear coupling between oscillators.

Historically, many different approaches have been taken as employing time dependant masses to give explicit time dependency to the Hamiltonian [2, 3], complex variable canonical quantisation similar to the Fokker-Plank equation [4] or using stochastic quantisation procedures [5]. However this proposals usually violated quantum constrains such as the uncertainty principle or the superposition principle, also being only able to describe a very restricted amount of cases.

One of the most successful and intuitive approaches has been the use of a large system composed of constituents that obey the canonical quantisation rules and where friction emerges from the energy transfer from the system to the environment.

In specific, system and reservoir methods are a popular and useful way to study these open quantum systems and can be broadly divided into two categories: By use of the Schrödinger picture one can find the generalised master equation for the density operator [6, 7, 8] or through the Heisenberg picture a Langevin equation approach is found to give proper description to the particular operators of the system [9, 10]. Albeit the interaction picture is also useful under the right circumstances [11].

Quantum master equations can be very useful tools with applications in a wide variety of cases, taking most quantum phenomena into account. However, they prove to be unsuccessful when the Born approximation is not feasible or the Markov assumption is violated.

In our case, we will focus on the Heisenberg picture approach as our interest is to obtain an exact result due to the use of harmonic forces [9] as a way of introduction to this field. This specific approach however is not able to describe unharmonic potentials required for, for example, quantum tunnelling [12]. Thus, this type of phenomena will be left out of the scope of this study.

Thus, the formalism employed in this work will consider a system of oscillators connected through harmonic coupling to their first neighbours in a one dimensional fashion, a chain of oscillators. The environment will be introduced in the model through the use of baths connected to the oscillators which will follow the Caldeira-Legget model. The spectral densities considered will be ohmic ($\propto \omega$, linear with the frequency) and super ohmic ($\propto \omega^s$, $s > 1$).

The Caldeira-Legget model is a semi-empirical model where the system of interest is coupled to a bath or environment which is defined as a infinite collection of non interacting harmonic oscillators [13, 14]. While conceptually simple, this model requires to know the properties of the closed system of interest, the quantum oscillator chain in our case, as well as the form of interaction between the oscillator and the bath. The spectral density of the bath is introduced as a way to describe this interaction and the bath completely. The advantage of this model is that it reflects the mechanics of a realistic dissipative system and can be treated analytically while avoiding usual problems of the canonical quantisation.

As we are going to use the Langevin formalism, it might be practical to introduce it through the lenses of the classical approach to describe the strengths and difficulties of said formalism. In a classical Langevin equation the dynamics of the system are primary determined by the environment through the friction and stochastic forces [15]. One might also take into account the memory kernel of the system in case the friction force is retarded, but usually it is applied as a linear force also local in time. Assuming no memory and no frequency dependence on the stochastic force (white noise), the Langevin equation can be expressed for a 1D system as

$$\ddot{q}(t) + \gamma \dot{q}(t) + \frac{1}{m} \frac{dV(q)}{dq} = \frac{\xi(t)}{m}, \tag{1.0.1}$$

where m is the particle mass, $q(t)$ is the position, γ is usually regarded as the friction or damping coefficient, $V(q)$ is a potential and thus it's derivative acts as an external force and $\xi(t)$ is the stochastic force. The friction term is usually referred to as an ohmic term due to the linear dependence with the velocity in analogy to its counterpart in circuit theory, the resistor. This equation can describe the movement of a Brownian particle immersed in a fluid of light particles [15]. If we want to study systems with a reservoir with coloured noise and memory, the dynamics can be portrayed using the following generalised equation

$$\ddot{q}(t) + \int_{-\infty}^{t} dt' \gamma(t - t') \dot{q}(t') + \frac{1}{m} \frac{dV(q)}{dq} = \frac{\xi(t)}{m}. \tag{1.0.2}$$

The term $\gamma(t-t')$ is usually regarded as the memory kernel. Its dependence with $t-t'$ is useful as we can use the convolution theorem to obtain the stationary memory kernel under steady state conditions [16]. The stochastic force vanishes on average but it is relevant as its auto-correlation function is important for the fluctuation dissipation relation through the Green-Kubo Formula, which will give us a way to determine the nature of the frequency-dependant damping coefficient $\tilde{\gamma}(\omega)$.

One important limitation in the classic regime is the time scale, where we need the system to evolve to at least a time comparable to that of the memory of the reservoir (that is, to $\frac{1}{\gamma}$). That being said, one could expect that at sufficiently low temperatures quantum effects take over and a different description of the dissipation can be achieved. However, this step is not without difficulty, as we now need to find a way to use the canonical scheme of quantisation for the Hamiltonian of the system in order to obtain the proper dissipation dynamics expected in the classic regime.

Thus, for our case of study we will need to fully understand both the Langevin formalism and the interaction with the baths. We will only consider a memorials approach and the influence of the bath over the coordinates of the oscillators will have to be taken into account as correction for their effective natural frequencies. This will be done under a renormalisation scheme described in detail in the text. Afterwards, the equations of motion will give us a way to solve the relation between baths and oscillators and the use of the fluctuation dissipation relation, central in the Langevin formalism, will give us the key to express all our properties of interest as analytical terms of the covariance matrix at the steady state.

However, under this approach the analytical description of larger systems than a two oscillator case requires the use of $N \times N$ matrix operations and the only way to study them properly is to use numerical calculations. Due to the nature of this calculations large systems

tend to be quite costly in terms of performance, making the analysis of very long chains an important compromise.

The aim of this work is to study 1D quantum systems at the steady state under a system plus reservoir model, specifically using the Caldeira-Legget bath model, from a numerical point of view. We review the implications of tuning different parameters and constraints of the system such as the spectral density of the baths, the coupling between the oscillators or the temperature profile. To do so we will obtain the elements of the covariance matrix and subsequently the heat currents of the baths. This will allow us to analyse the energy transport under different circumstances and also to observe the interaction between different ends of the chain under specific conditions, such as the absence of coupling among oscillators on the same bath.

In specific, we split the analysis in two main scenarios.

1. A system connected to a single bath. The relevance of this scenario is the characterisation of the equilibrium steady state by means of the covariance matrix.

2. A system with multiple baths, where each element of the chain can be connected to only one bath. The aim now is to review the properties outside of the equilibrium of the steady state by means of assigning different temperatures to the baths. We will study properties such as the temperature profile or the heat currents expressed through the elements of the covariance matrix. Thus, the parameters of the system will give characteristic behaviours to this properties. Among this parameters we have the coupling between oscillators or oscillators with the baths. The spectral density of the baths will also be of utmost importance, as we will see.

The following text is divided into three chapters and three appendices. The first chapter studies the general framework required for the rest of this work, a chain of linearly coupled oscillators connected to Caldeira-Legget model baths. The covariance matrix elements expressions will be obtained and from there the properties of the system will be formulated. The following chapter will talk about specific cases of interest of this model under different constrains with a progressive evolution from simpler to more complicated scenarios. We will find the classical limit of the system as well as interesting results for a broken chain with no coupling among the oscillators of the same bath. The last chapter will sum up the findings in the work and showcase the possibilities of this system for further research.

The appendices will describe auxiliary results needed throughout this work as well as a description of the numerical procedure used to calculate the integrals of the elements in the covariance matrix.

Chapter 2

Chain of linearly coupled oscillators with Caldeira-Legget baths
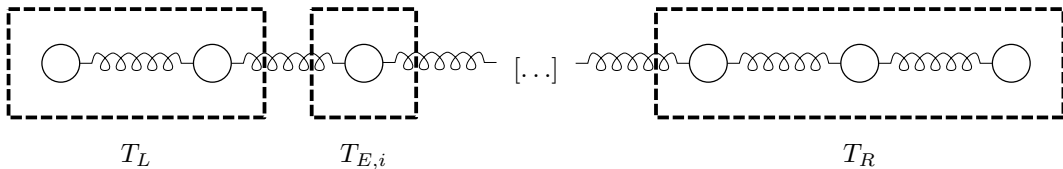

Figure 2.1: General set up for the chain of linearly coupled oscillators. The circles represent the oscillators. The springs represent the linear harmonic coupling between first neighbours. The dashed line boxes represent the baths and their interaction with the oscillators on their interior. Temperature labels are assigned for each bath.

The model under study is based on a chain of oscillators connected through a pairwise harmonic potential, which represent the system, and a certain amount of reservoirs or baths that represent the environment. A diagram of this model can be seen in figure 2.1 where the springs illustrate the harmonic coupling and the dashed boxes the particular baths connected to the oscillators. We will consider that all oscillators in the chain can only be directly influenced by one bath each. Then, if for every bath α there is a N_α number of oscillators, $N = \sum_\alpha N_\alpha$. The equilibrium distance between neighbours will be considered to be equal for all of them. Thus we define $\hat{x}_i$ as the displacement from the equilibrium position and $\hat{p}_i$ as the corresponding moment for each oscillator. We also decompose the total Hamiltonian in three terms, $\hat{H}_S$ as the Hamiltonian of the closed system, $\hat{H}_B$ as the Hamiltonian of the baths and $\hat{H}_{SB}$ as the interaction between the baths and the system. Notice that here we define $H_{S,\text{bare}}$ as we will find the *renormalised* Hamiltonian later on.

$$\hat{H}_{S,\text{bare}} = \sum_{i=1}^{N} \frac{\hat{p}_i^2}{2m_i} + \frac{1}{2}m_i\omega_i^2\hat{x}_i^2 + \hat{V}(\hat{x}_i, \hat{x}_{i+1}), \qquad (2.0.1)$$

with

$$\hat{V}(\hat{x}_i, \hat{x}_{i+1}) = \frac{1}{2}k_{i,i+1}(\hat{x}_i - \hat{x}_{i+1})^2. \qquad (2.0.2)$$

and

$$\hat{H}_B = \sum_\alpha \hat{H}_{B,\alpha} = \sum_\alpha \sum_{\mu_\alpha} \frac{\hat{p}_{\mu_\alpha}^2}{2m_{\mu_\alpha}} + \frac{1}{2} m_{\mu_\alpha} \omega_{\mu_\alpha}^2 \hat{x}_{\mu_\alpha}^2, \tag{2.0.3}$$

$$\hat{H}_{SB} = \sum_{i=1}^N \hat{x}_i \sum_\alpha c_{i,\alpha} \hat{B}_\alpha = \sum_{i=1}^N \hat{x}_i \sum_\alpha c_{i,\alpha} \sum_{\mu_\alpha} g_{\mu_\alpha} \hat{x}_{\mu_\alpha}, \tag{2.0.4}$$

where

$$c_{i,\alpha} = 1; \text{ if osc. } i \text{ is connected to bath } \alpha, \tag{2.0.5}$$

$$c_{i,\alpha} = 0; \text{ if osc. } i \text{ is not connected to bath } \alpha. \tag{2.0.6}$$

μ_α is the index for the oscillators that compose the bath α, making $m_{\mu_\alpha}, \omega_{\mu_\alpha}$ the mass and natural frequency and $\hat{x}_{\mu_\alpha}, \hat{p}_{\mu_\alpha}$ the position and momentum of this oscillators respectively.

In general $\hat{B}_\alpha$ is an operator that describes the interaction of the system with the bath α. In this work we will only consider a linear relation between the spatial coordinate $\hat{x}_i$ and the spatial coordinate of the oscillators in the bath $\hat{x}_{\mu_\alpha}$. In this case, $\hat{B}_\alpha = \sum_{\mu_\alpha} g_{\mu_\alpha} \hat{x}_{\mu_\alpha}$.

This will help us solve the equations of motion as the linear terms are trivial to derive and operate with. This is important in order to arrive at a *simple* solution for the covariance matrix in the steady state.

2.1 Re-normalisation of the Hamiltonian

If we separate the Hamiltonian into potential and kinetic terms, we can define the potential term as:

$$\hat{W}(\{\hat{x}_i\}, \{\hat{x}_{\mu_\alpha}\}) = \sum_\alpha \sum_{\mu_\alpha} \frac{1}{2} m_{\mu_\alpha} \omega_{\mu_\alpha}^2 \hat{x}_{\mu_\alpha}^2 + \sum_{i=1}^N \hat{x}_i \sum_\alpha c_{i,\alpha} \sum_{\mu_\alpha} g_{\mu_\alpha} \hat{x}_{\mu_\alpha} + \sum_{i=1}^N \frac{1}{2} m_i \omega_i^2 \hat{x}_i^2 + \hat{V}(\hat{x}_i, \hat{x}_{i+1}). \tag{2.1.1}$$

Equation 2.1.1 can be minimised with respect to the positions of the oscillators of the bath α yielding the following result:

$$\hat{x}_{\mu_\alpha}^* = -\frac{1}{m_{\mu_\alpha} \omega_{\mu_\alpha}^2} \sum_{i=1}^N \hat{x}_i c_{i,\alpha} g_{\mu_\alpha}. \tag{2.1.2}$$

$\hat{x}_{\mu_\alpha}^*$ minimises the effect of the bath over the oscillators, showcasing the direct influence of the bath as a potential. Notice that this affects the high temperature limit of the steady state in comparison with the corresponding thermal state, which is only dependent on the kinetic term and thus the potential term might become relevant for large values of g_{μ_α}. Thus, we remove this contribution from the original Hamiltonian to preserve the high temperature limit.

$$\hat{H}_{S,\text{bare}} - \hat{W}(\{\hat{x}_i\}, \{\hat{x}_{\mu_\alpha}^*\}) = \sum_{i=1}^N \frac{m_i}{2} \Omega_i^2 \hat{x}_i^2 - k_{i,i+1} \hat{x}_i \hat{x}_{i+1} + \frac{1}{2} \sum_{i=1}^N \sum_{j=1, j\neq i}^N K_{ij} \hat{x}_i \hat{x}_j.$$

Where we have defined the following terms:

$$K_\alpha = \sum_{\mu_\alpha} \frac{g_{\mu_\alpha}^2}{m_{\mu_\alpha} \omega_{\mu_\alpha}^2}, \tag{2.1.3}$$

$$K_{ij} = K_{ji} = \sum_\alpha K_\alpha c_{i,\alpha} c_{j,\alpha}, \tag{2.1.4}$$

$$\Omega_i^2 = \omega_i^2 + \frac{k_{i,i+1} + k_{i-1,i}}{m_i} + \sum_\alpha (c_{i,\alpha})^2 \frac{K_\alpha}{m_i}. \tag{2.1.5}$$

Thus, the Hamiltonian for the oscillators turns into:

$$\hat{H}_S = \sum_{i=1}^N \frac{\hat{p}_i^2}{2m_i} + \sum_{i=1}^N \frac{m_i}{2} \Omega_i^2 \hat{x}_i^2 - k_{i,i+1} \hat{x}_i \hat{x}_{i+1} + \frac{1}{2} \sum_{i=1}^N \sum_{j=1,j\neq i}^N K_{ij} \hat{x}_i \hat{x}_j. \tag{2.1.6}$$

So that the final Hamiltonian is

$$\hat{H} = \hat{H}_S + \hat{H}_B + \hat{H}_{SB}. \tag{2.1.7}$$

2.2   Equations of motion

Now we obtain the equations of motion for the operators of the oscillator, as well as for the bath coordinates in order to deduce later the covariance matrix. To do so we will assume that the operators do not depend explicitly on time, so that by means of Heisenberg's picture we can use the following result:

$$\frac{d\hat{O}}{dt} = \frac{i}{\hbar}[\hat{H}, \hat{O}]. \tag{2.2.1}$$

for any operator $\hat{O}$. We also make use of the following relations:

$$[\hat{x}_i, \hat{p}_j] = i\hbar \delta_{ij}, \tag{2.2.2}$$

$$[\hat{x}_i^2, \hat{p}_j] = 2i\hbar \hat{x}_i \delta_{ij}, \tag{2.2.3}$$

$$[\hat{x}_i, \hat{p}_j^2] = 2i\hbar \hat{p}_i \delta_{ij}. \tag{2.2.4}$$

2.2.1   Equations for the oscillators

Particularising 2.2.1 for the operators of the oscillators we obtain:

$$\frac{d\hat{x}_i}{dt} = \frac{\hat{p}_i}{m_i}, \tag{2.2.5}$$

$$\frac{d\hat{p}_i}{dt} = \frac{i}{\hbar}[\hat{H}, \hat{p}_i] = \frac{i}{\hbar}[\hat{H}_S, \hat{p}_i] + \frac{i}{\hbar}[\hat{H}_{SB}, \hat{p}_i]. \tag{2.2.6}$$

For the first commutator we have:

$$\frac{i}{\hbar}[\hat{H}_S, \hat{p}_i] = -m_i \Omega_i^2 \hat{x}_i + (k_{i,i+1} \hat{x}_{i+1} + k_{i-1,i} \hat{x}_{i-1}) - \sum_{j=1,j\neq i}^N K_{ij} \hat{x}_j. \tag{2.2.7}$$

As for the second commutator:

$$\frac{i}{\hbar}[\hat{H}_{SB}, \hat{p}_i] = -\sum_\alpha c_{i,\alpha} \sum_{\mu_\alpha} g_{\mu_\alpha} \hat{x}_{\mu_\alpha}. \tag{2.2.8}$$

Then:

$$\frac{d\hat{p}_i}{dt} = -m_i \Omega_i^2 \hat{x}_i + k_{i,i+1} \hat{x}_{i+1} + k_{i-1,i} \hat{x}_{i-1} - \sum_{j=1,j\neq i}^N K_{ij} \hat{x}_j - \sum_\alpha c_{i,\alpha} \sum_{\mu_\alpha} g_{\mu_\alpha} \hat{x}_{\mu_\alpha}. \tag{2.2.9}$$

To solve (2.2.9) we need to get rid of the coordinates of the oscillators of the baths ($\hat{x}_{\mu_\alpha}$) so we calculate the equations of motion for said operators.

2.2.2 Equations for the baths

In the same fashion we introduce the bath oscillators operators on 2.2.1 to obtain the following.

$$\frac{d\hat{x}_{\mu_\alpha}}{dt} = \frac{\hat{p}_{\mu_\alpha}}{m_{\mu_\alpha}}, \tag{2.2.10}$$

$$\frac{d\hat{p}_{\mu_\alpha}}{dt} = \frac{i}{\hbar}[\hat{H}, \hat{p}_{\mu_\alpha}] = -m_{\mu_\alpha} \omega_{\mu_\alpha}^2 \hat{x}_{\mu_\alpha} - g_{\mu_\alpha} \sum_{i=1}^N c_{i,\alpha} \hat{x}_i. \tag{2.2.11}$$

We combine these two equations to obtain:

$$m_{\mu_\alpha} \ddot{\hat{x}}_{\mu_\alpha} + m_{\mu_\alpha} \omega_{\mu_\alpha}^2 \hat{x}_{\mu_\alpha} = -\sum_{i=1}^N c_{i,\alpha} g_{\mu_\alpha} \hat{x}_i. \tag{2.2.12}$$

Applying a Laplace transform to 2.2.12 and taking into account the known results in appendix B.1 now we can determine $\hat{x}_{\mu_\alpha}(t)$ assuming that we know the initial state of the oscillators of the baths.

$$L(\hat{x}_{\mu_\alpha}) = \frac{s}{s^2 + \omega_{\mu_\alpha}^2} \hat{x}_{\mu_\alpha}(t_0) + \frac{1}{s^2 + \omega_{\mu_\alpha}^2} \dot{\hat{x}}_{\mu_\alpha}(t_0) - \sum_{i=1}^N c_{i,\alpha} \frac{g_{\mu_\alpha}}{m_{\mu_\alpha}} \frac{L(\hat{x}_i)}{s^2 + \omega_{\mu_\alpha}^2}. \tag{2.2.13}$$

Now we apply the inverse Laplace transform to obtain an explicit expression with time

$$\hat{x}_{\mu_\alpha}(t) = \hat{x}_{\mu_\alpha}(t_0) \cos(\omega_{\mu_\alpha}(t - t_0)) + \frac{\hat{p}_{\mu_\alpha}(t_0)}{m_{\mu_\alpha} \omega_{\mu_\alpha}} \sin(\omega_{\mu_\alpha}(t - t_0))$$

$$-\sum_{i=1}^N c_{i,\alpha} \frac{g_{\mu_\alpha}}{m_{\mu_\alpha} \omega_{\mu_\alpha}} \int_{t_0}^t dt' \sin(\omega_{\mu_\alpha}(t - t')) \hat{x}_i(t'). \tag{2.2.14}$$

2.2.3 Correspondence between coordinates and bath terms

Now we have the description of the coordinates of the baths in terms of time evolution terms and the coordinates of the oscillators connected to said baths, as showcased in (2.2.14). To solve (2.2.9) we first calculate $\sum_{\mu_\alpha} g_{\mu_\alpha} \hat{x}_{\mu_\alpha}$ and then replace the result in said equation.

$$\sum_{\mu_\alpha} g_{\mu_\alpha} \hat{x}_{\mu_\alpha} = \sum_{\mu_\alpha} \left(g_{\mu_\alpha} \hat{x}_{\mu_\alpha}(t_0) \cos(\omega_{\mu_\alpha}(t - t_0)) + \frac{g_{\mu_\alpha} \hat{p}_{\mu_\alpha}(t_0)}{m_{\mu_\alpha} \omega_{\mu_\alpha}} \sin(\omega_{\mu_\alpha}(t - t_0)) \right)$$

$$- \sum_{i=1}^{N} c_{i,\alpha} \sum_{\mu_\alpha} \frac{g_{\mu_\alpha}^2}{m_{\mu_\alpha} \omega_{\mu_\alpha}} \int_{t_0}^{t} dt' \sin(\omega_{\mu_\alpha}(t - t')) \hat{x}_i(t'). \tag{2.2.15}$$

We can always include a step function to extend the limit of the integral to infinity, such that $\int_{t_0}^{t} f(t')dt' = \int_{t_0}^{\infty} f(t')\Theta(t - t')dt'$ and we will also assume that $t_0 \to -\infty$. Also notice how the first sum is independent of any coordinates and only depends on time, the initial conditions and the parameters of the bath.

$$\sum_{\mu_\alpha} g_{\mu_\alpha} \hat{x}_{\mu_\alpha} = \sum_{\mu_\alpha} \left(g_{\mu_\alpha} \hat{x}_{\mu_\alpha}(t_0) \cos(\omega_{\mu_\alpha}(t - t_0)) + \frac{g_{\mu_\alpha} \hat{p}_{\mu_\alpha}(t_0)}{m_{\mu_\alpha} \omega_{\mu_\alpha}} \sin(\omega_{\mu_\alpha}(t - t_0)) \right)$$

$$- \sum_{i=1}^{N} c_{i,\alpha} \int_{-\infty}^{\infty} dt' \left[\sum_{\mu_\alpha} \frac{g_{\mu_\alpha}^2}{m_{\mu_\alpha} \omega_{\mu_\alpha}} \sin(\omega_{\mu_\alpha}(t - t'))\Theta(t - t') \right] \hat{x}_i(t'). \tag{2.2.16}$$

We will rewrite equation 2.2.16 with the following definitions:

$$f_\alpha(t) = -\sum_{\mu_\alpha} \left[g_{\mu_\alpha} \hat{x}_{\mu_\alpha}(t_0) \cos(\omega_{\mu_\alpha}(t - t_0)) + \frac{g_{\mu_\alpha} \hat{p}_{\mu_\alpha}(t_0)}{m_{\mu_\alpha} \omega_{\mu_\alpha}} \sin(\omega_{\mu_\alpha}(t - t_0)) \right], \tag{2.2.17}$$

$$d_\alpha(t) = \sum_{\mu_\alpha} \frac{g_{\mu_\alpha}^2}{m_{\mu_\alpha} \omega_{\mu_\alpha}} \sin(\omega_{\mu_\alpha} t)\Theta(t). \tag{2.2.18}$$

So that

$$\sum_{\mu_\alpha} g_{\mu_\alpha} \hat{x}_{\mu_\alpha} = -f_\alpha(t) - \sum_{i=1}^{N} c_{i,\alpha} d_\alpha(t) * \hat{x}_i. \tag{2.2.19}$$

Now we use equation 2.2.19 to properly solve 2.2.9.

$$m_i \ddot{\hat{x}}_i(t) = - m_i \Omega_i^2 \hat{x}_i(t) + k_{i,i+1} \hat{x}_{i+1}(t) + k_{i-1,i} \hat{x}_{i-1}(t)$$

$$- \sum_{j=1, j \neq i}^{N} K_{ij} \hat{x}_j(t) + \sum_\alpha c_{i,\alpha} \left(f_\alpha(t) + \sum_{k=1}^{N} c_{k,\alpha} d_\alpha(t) * \hat{x}_k(t) \right). \tag{2.2.20}$$

One can compare the terms in equation 2.2.20 to the classic Langevin equation 1.0.2 to see the correspondence to the classical scenario. The left side of the equation corresponds to the total force applied to the oscillator i at time t, the first four terms on the right side come from potential terms and $f_\alpha(t)$ is analogous to the stochastic force. The explicit form of the friction term is hidden under the convolution $d_\alpha(t) * \hat{x}_k(t)$ since

$$d_\alpha(t) * \hat{x}_k(t) = \int_{-\infty}^{\infty} dt' d_\alpha(t - t') \hat{x}_i(t'). \tag{2.2.21}$$

Applying a Fourier transform to equation 2.2.20 and using the properties shown in appendix B.2, we find a direct relationship between $\hat{X}_i(\omega) = F[\hat{x}_i(t)]$ and $\hat{G}_i(\omega) = F[\sum_\alpha c_{i,\alpha} \hat{f}_\alpha(t)]$:

$$m_i \left(\Omega_i^2 - \omega^2 - \sum_\alpha (c_{i,\alpha})^2 \frac{D_\alpha}{m_i} \right) \hat{X}_i$$

$$+ \sum_{j=1, j \neq i}^{N} \left(\sum_\alpha c_{i,\alpha} c_{j,\alpha} (K_\alpha - D_\alpha) - k_{j,i}\delta_{j,i-1} - k_{i,j}\delta_{j,i+1} \right) \hat{X}_j = \sum_\alpha c_{i,\alpha} \hat{F}_\alpha = \hat{G}_i. \tag{2.2.22}$$

where $D_\alpha(\omega) = F[d_\alpha(t)]$. D_α will be properly explored on the following section, for now we leave it's discussion for later. If we define a vector such as $\hat{X} = (\hat{X}_1, \dots, \hat{X}_N)^T$ and $\hat{G} = (\hat{G}_1, \dots, \hat{G}_N)^T$ then we can turn (2.2.22) into a matrix operation and inverse said matrix, let us call it $M(\omega)$, so that the inverse matrix $A(\omega)$ is multiplying the vector $\hat{G}$.

$$M(\omega)\hat{X}(\omega) = \hat{G}(\omega) \implies \hat{X}(\omega) = M^{-1}(\omega)\hat{G}(\omega) = A(\omega)\hat{G}(\omega). \qquad (2.2.23)$$

Then

$$\hat{X}_i(\omega) = \sum_j A_{ij}(\omega)\hat{G}_j(\omega). \qquad (2.2.24)$$

Here we can infer some interesting properties of the matrix A which might prove relevant for numerical calculations.

Since $D_\alpha(\omega) = F[d_\alpha(t)] = \int_{-\infty}^{\infty} dt e^{i\omega t} d_\alpha(t)$ and $d_\alpha(t)$ is real, we have

$$D_\alpha(-\omega) = D_\alpha^*(\omega) \iff M(-\omega) = M^*(\omega) \iff A(-\omega) = A^*(\omega) \qquad (2.2.25)$$

Then

$$\mathrm{Re}[A_{ij}(-\omega)] = \mathrm{Re}[A_{ij}(\omega)], \qquad (2.2.26)$$

$$\mathrm{Im}[A_{ij}(-\omega)] = -\mathrm{Im}[A_{ij}(\omega)]. \qquad (2.2.27)$$

2.2.4 Covariance Matrix

We can obtain the covariance matrix making use of the fluctuation dissipation relation

$$\frac{1}{2}\langle\{\hat{F}_\alpha(\omega), \hat{F}_\alpha(\omega')\}\rangle = 2\pi\hbar\delta(\omega + \omega')\coth\left(\frac{\hbar\omega}{2K_B T_\alpha}\right)\mathrm{Im}[D_\alpha(\omega)], \qquad (2.2.28)$$

which resolution can be found on Appendix A.

The covariance matrix σ is defined using the vector of the coordinates of the system, defined in this case as $\vec{R} = (x_1, p_1, \dots, x_i, p_i, \dots, x_N, p_N)^T$ which elements are defined as $\sigma_{ij}(t, t') = \frac{1}{2}\langle\{R_i(t), R_j(t')\}\rangle$. In our study we will focus on the asymptotic state of the system, so we define the steady state at the limit where $t_0 \to -\infty$. We also particularise the correlations to the case $t' = t$ so as to obtain the elements of the covariance matrix.

With this we can easily define the elements of the covariance matrix making use of 2.2.24, 2.2.28. We begin with σ_{x_i, x_j}:

$$
\begin{aligned}
\frac{1}{2}\langle\{\hat{x}_i(t), \hat{x}_j(t')\}\rangle &= \frac{1}{2}\frac{1}{2\pi}\int_{-\infty}^{\infty} d\omega e^{-i\omega t}\frac{1}{2\pi}\int_{-\infty}^{\infty} d\omega' e^{-i\omega' t'}\langle\{\hat{X}_i(\omega), \hat{X}_j(\omega')\}\rangle \\
&= \frac{1}{8\pi^2}\int_{-\infty}^{\infty} d\omega e^{-i\omega t}\int_{-\infty}^{\infty} d\omega' e^{-i\omega' t'}\sum_{k=1}^{N} A_{ik}(\omega)\sum_{l=1}^{N} A_{jl}(\omega') \\
&\quad \cdot \langle\{\hat{G}_k(\omega), \hat{G}_l(\omega')\}\rangle \\
&= \frac{\hbar}{2\pi}\int_{-\infty}^{\infty} d\omega e^{-i\omega(t-t')}\sum_{k=1}^{N} A_{ik}(\omega)\sum_{l=1}^{N} A_{jl}(-\omega) \\
&\quad \cdot \sum_\alpha c_{k,\alpha}c_{l,\alpha}\coth\left(\frac{\hbar\omega}{2K_B T_\alpha}\right)\mathrm{Im}[D_\alpha(\omega)]. \qquad (2.2.29)
\end{aligned}
$$

If we now consider $t' = t$ we obtain σ_{x_i, x_j}:

$$\sigma_{x_i,x_j} = \frac{\hbar}{2\pi} \int_{-\infty}^{\infty} d\omega \sum_{k=1}^{N} \sum_{l=1}^{N} A_{ik}(\omega) A_{jl}(-\omega) \sum_{\alpha} c_{k,\alpha} c_{l,\alpha} \coth\left(\frac{\hbar\omega}{2K_B T_\alpha}\right) \text{Im}[D_\alpha(\omega)].$$

(2.2.30)

We can find the rest of the elements with the same procedure, taking into account that $F[\hat{p}_i] = -im_i\omega\hat{X}_i$. The remaining elements of the covariance matrix will follow the patterns:

$$\sigma_{x_i,p_j} = \frac{i\hbar}{2\pi} m_j \int_{-\infty}^{\infty} d\omega\, \omega \sum_{k=1}^{N} \sum_{l=1}^{N} A_{ik}(\omega) A_{jl}(-\omega) \sum_{\alpha} c_{k,\alpha} c_{l,\alpha} \coth\left(\frac{\hbar\omega}{2K_B T_\alpha}\right) \text{Im}[D_\alpha(\omega)],$$

(2.2.31)

$$\sigma_{p_i,x_j} = -\frac{i\hbar}{2\pi} m_i \int_{-\infty}^{\infty} d\omega\, \omega \sum_{k=1}^{N} \sum_{l=1}^{N} A_{ik}(\omega) A_{jl}(-\omega) \sum_{\alpha} c_{k,\alpha} c_{l,\alpha} \coth\left(\frac{\hbar\omega}{2K_B T_\alpha}\right) \text{Im}[D_\alpha(\omega)],$$

(2.2.32)

$$\sigma_{p_i,p_j} = \frac{\hbar}{2\pi} m_i m_j \int_{-\infty}^{\infty} d\omega\, \omega^2 \sum_{k=1}^{N} \sum_{l=1}^{N} A_{ik}(\omega) A_{jl}(-\omega) \sum_{\alpha} c_{k,\alpha} c_{l,\alpha} \coth\left(\frac{\hbar\omega}{2K_B T_\alpha}\right) \text{Im}[D_\alpha(\omega)].$$

(2.2.33)

We can employ the relations 2.2.26, 2.2.27 to reduce the terms of the sum, as we can get rid of certain products due to parity.

$$\begin{aligned} A_{ik}(\omega) A_{jl}(-\omega) =& \text{Re}[A_{ik}(\omega)]\text{Re}[A_{jl}(\omega)] + \text{Im}[A_{ik}(\omega)]\text{Im}[A_{jl}(\omega)] \\ &+ i\left(\text{Im}[A_{ik}(\omega)]\text{Re}[A_{jl}(\omega)] - \text{Re}[A_{ik}(\omega)]\text{Im}[A_{jl}(\omega)]\right). \end{aligned}$$

Since the integral has to be real as the covariance matrix elements are real as well, we can discard half of these terms in the sum depending on the matrix element. Also, the imaginary part will be zero when all indices are the same or at least paired so that $i = j, k = l$. Parity also plays an important part as this product decides the parity of the integrand in combination with the corresponding ω term $(1, \omega, \omega^2)$. The integrand must be even for the result to be different from zero, taking into account that $\text{Im}[D_\alpha(\omega)]$ and $\coth\left(\frac{\hbar\omega}{2K_B T}\right)$ are both odd and thus their product is even.

Moreover, taking a closer look at equations 2.2.31, 2.2.32 and since by definition $\sigma_{x_i,p_i} = \sigma_{p_i,x_i}$ one obtains

$$\sigma_{x_i,p_i} = \sigma_{p_i,x_i} = 0. \tag{2.2.34}$$

2.2.5 Oscillator Temperature

In order to define the temperature profile of the chain, which will give us important information about the system, we need to define some kind of temperature measurement for each oscillator. We will rely on the equipartition theorem and the canonical quantisation scheme to define the local kinetic temperature of each oscillator as

$$\tau_i = \frac{\sigma_{p_i,p_i}}{k_B m_i}, \tag{2.2.35}$$

since we assume $\frac{1}{2}k_B\tau_i = \langle\frac{\hat{p}_i^2}{2m_i}\rangle$ as we only have one degree of freedom in $\hat{x}_i$ and $\sigma_{p_i,p_i} = \frac{1}{2}(\hat{p}_i\hat{p}_i + \hat{p}_i\hat{p}_i) = \hat{p}_i^2$.

It is important to highlight that this is a kinetic temperature and doesn't take into account the potential part of the Hamiltonian. When the interaction terms become more relevant τ_i will not be a proper characterisation of the temperature of the oscillator i.

2.2.6 Heat Currents

We can also define the heat current in order to study the energy exchange between the oscillators, which gains interest for bigger systems. Since we are studying the energy exchange and our system is isolated, due to no external driving inducing work on the system, we can identify $\frac{d}{dt}\langle \hat{H}_S \rangle = \sum_\alpha \dot{Q}_\alpha$. One can quickly perceive $\dot{Q}_\alpha$ as the energy change in form of heat induced by the coupling with each bath α. Thus, the global and local heat currents can be calculated solving $\frac{d}{dt}\langle \hat{H}_S \rangle$.

$$\frac{d}{dt}\langle \hat{H}_S \rangle = \frac{i}{\hbar}\langle [\hat{H}, \hat{H}_S] \rangle = \frac{i}{\hbar}\langle [\hat{H}_{SB}, \hat{H}_S] \rangle = \frac{i}{\hbar}\langle \left[\sum_i \hat{x}_i \sum_\alpha c_{i,\alpha} \sum_{\mu_\alpha} g_{\mu_\alpha}\hat{x}_{\mu_\alpha}, \sum_j \frac{\hat{p}_j^2}{2m_j} \right] \rangle$$

$$= -\sum_\alpha \sum_i c_{i,\alpha}\frac{1}{m_i}\sum_{\mu_\alpha} g_{\mu_\alpha}\langle \hat{p}_i\hat{x}_{\mu_\alpha} \rangle. \tag{2.2.36}$$

Then

$$\dot{Q}_\alpha = -\sum_i c_{i,\alpha}\frac{1}{m_i}\sum_{\mu_\alpha} g_{\mu_\alpha}\langle \hat{p}_i\hat{x}_{\mu_\alpha} \rangle. \tag{2.2.37}$$

where α represents one of the baths in the system. By using the equation of motion for the ith oscillator (2.2.9) in order to replace $\sum_{\mu_\alpha} g_{\mu_\alpha}\hat{x}_{\mu_\alpha}$ and rewriting the expression in terms of the covariance matrix, we can get the desired result.

$$\dot{Q}_\alpha = \sum_i c_{i,\alpha}\frac{1}{m_i}\left[\langle \hat{p}_i\dot{\hat{p}}_i \rangle + \langle \hat{p}_i\hat{x}_i \rangle m_i\Omega_i^2 - k_{i,i+1}\langle \hat{p}_i\hat{x}_{i+1} \rangle - k_{i-1,i}\langle \hat{p}_i\hat{x}_{i-1} \rangle + \sum_{j=1,j\neq i}^{N} K_{ij}\langle \hat{p}_i\hat{x}_j \rangle \right]$$
$$\tag{2.2.38}$$

where $c_{i,\alpha}\sum_{\mu_\alpha} g_{\mu_\alpha}\hat{x}_{\mu_\alpha}$ has been obtained by multiplying (2.2.9) by $c_{i,\alpha}$.

We first solve each expected value making use of the following result:

$$[\hat{p}_i, \dot{\hat{p}}_j] = i\hbar m_i\Omega_i^2\delta_{ij}. \tag{2.2.39}$$

This is easily obtained through 2.2.9 as well. With this:

$$\langle \hat{p}_i\dot{\hat{p}}_i \rangle = \frac{1}{2}\langle \hat{p}_i\dot{\hat{p}}_i + \hat{p}_i\dot{\hat{p}}_i \rangle = \frac{d}{dt}\sigma_{p_i,p_i} + \frac{1}{2}i\hbar m_i\Omega_i^2, \tag{2.2.40}$$

$$\langle \hat{p}_i\hat{x}_i \rangle = \frac{1}{2}\langle \hat{p}_i\hat{x}_i + \hat{p}_i\hat{x}_i \rangle = \frac{1}{2}\sigma_{p_ix_i} - \frac{1}{2}i\hbar, \tag{2.2.41}$$

$$\langle \hat{p}_i\hat{x}_j \rangle|_{j\neq i} = \frac{1}{2}\langle \hat{p}_i\hat{x}_j + \hat{p}_i\hat{x}_j \rangle = \sigma_{p_ix_j}. \tag{2.2.42}$$

Then (2.2.37) turns into

$$\dot{Q}_\alpha = \sum_{i=1}^{N} c_{i,\alpha}\frac{1}{m_i}\left(\frac{1}{2}\frac{d}{dt}\sigma_{p_i,p_i} + m_i\Omega_i^2\sigma_{p_i,x_i} + \sum_{j=1,j\neq i}^{N} S_{ij}\sigma_{p_i,x_j} \right), \tag{2.2.43}$$

where

$$S_{ij} = S_{ji} = -k_{ij}\delta_{j,i+1} - k_{ji}\delta_{j,i-1} + \sum_\alpha c_{i,\alpha}c_{j,\alpha}K_\alpha.$$

It is trivial to notice that at the steady state $\frac{d}{dt}\sigma_{p_i,p_i} = 0$ and taking into account equation 2.2.34 one obtains the following result for the steady state:

$$\dot{Q}_\alpha = \sum_{i=1}^{N} c_{i,\alpha}\frac{1}{m_i}\sum_{j=1,j\neq i}^{N} S_{ij}\sigma_{p_i,x_j}. \tag{2.2.44}$$

2.3 Spectral Density

2.3.1 Definition

One interesting object of study is the spectral density, a term that fully describes the required properties of the bath. We will use this as a tool for our analysis so we will review its definition and links to other elements present in the study of the bath.

We define the spectral density as

$$J_\alpha(\omega) = \pi \sum_{\mu_\alpha} \frac{g_{\mu_\alpha}^2}{2m_{\mu_\alpha}\omega_{\mu_\alpha}} \delta(\omega - \omega_{\mu_\alpha}). \tag{2.3.1}$$

With this expression it can be seen that J_α describes the interaction with the bath when the frequency is equal to the frequency of one of the oscillators of the bath. This can be easily extended for the continuum. We can make a Riemann sum and turn it into an integral.

$$\frac{\pi}{2} \sum_{\mu_\alpha} \frac{g_{\mu_\alpha}^2}{m_{\mu_\alpha}\omega_{\mu_\alpha}^2} \to \int_0^\infty \frac{J_\alpha(\omega)}{\omega} d\omega. \tag{2.3.2}$$

With this, we can rewrite (2.1.3) as

$$K_\alpha = \frac{2}{\pi} \int_0^\infty d\omega \frac{J_\alpha(\omega)}{\omega}. \tag{2.3.3}$$

2.3.2 Susceptibility

From equation 2.3.2 it follows that a Riemann sum will yield an expression for equation 2.2.18 that explicitly includes the spectral density.

$$d_\alpha(t) = \frac{2}{\pi} \int_0^\infty d\omega' J_\alpha(\omega') \sin(\omega't)\Theta(t). \tag{2.3.4}$$

This expression is also known as the dissipation kernel and it's Fourier transform is known as susceptibility.

As for the susceptibility, knowing the following Fourier transform result:

$$\text{Im}[F[\sin(\omega't)\Theta(t)]] = \frac{\pi}{2}[\delta(\omega - \omega') - \delta(\omega + \omega')] \tag{2.3.5}$$

we can separate the result in a real part and a imaginary part. For the imaginary part since $\omega' \in [0, \infty)$ we need to extend the limits of integration in order to obtain a result for $\delta(\omega + \omega')$. To do so we multiply the integrand by $\Theta(\omega')$ and extend the integration domain to $\omega' \in (-\infty, \infty)$. Finally:

$$\text{Im}[D_\alpha(\omega)] = J_\alpha(\omega)\Theta(\omega) - J_\alpha(-\omega)\Theta(-\omega). \tag{2.3.6}$$

As for the real part, the procedure is not so straight forward. Equation 2.3.5 is causal due to the Heaviside step function. Causal response functions have analytic Fourier transform in the upper half of the complex plane and therefore, the Kramers-Kronig relations hold [1]. In this case,

$$Re[D_\alpha(\omega)] = \frac{1}{\pi} P \int_{-\infty}^\infty d\omega' \frac{\text{Im}[D_\alpha(\omega')]}{\omega' - \omega}. \tag{2.3.7}$$

2.3.3 Spectral density examples

In this work we will focus on ohmic baths, which take their name from Ohm's Law since it arises from a damping force produced by a potential on the electrons that pass through a material. This analogy serves as reference to the behaviour of this baths, since they are in principle described as directly proportional to a damping constant γ and are linearly dependant on the frequency. We will use different cases with cut-offs such as the Drude Lorentz and a step function. We will also study a super-ohmic model, which is similar to an ohmic model but where the spectral density is proportional to the nth power of ω.

Drude Lorentz Model

This model employs a soft decay where the spectral density is modulated using a Lorentzian of the form $\frac{\Lambda^2}{\omega^2+\Lambda^2}$. The spectral density is defined as:

$$J_{DL}(\omega) = m\gamma\omega\frac{\Lambda^2}{\omega^2+\Lambda^2}. \tag{2.3.8}$$

First we obtain K_α using 2.3.3 resulting in

$$K_{DL} = \frac{2}{\pi}\int_0^\infty d\omega\frac{J_{DL}(\omega)}{\omega} = \frac{2}{\pi}m\gamma\int_0^\infty\frac{1}{1+\omega'^2}\Lambda d\omega' = m\gamma\Lambda, \tag{2.3.9}$$

where $\omega' = \frac{\omega}{\Lambda}$.

To calculate the corresponding susceptibility we use equations (2.3.6, 2.3.7) for the imaginary and real parts respectively.

As the imaginary part is just turning the spectral density into an odd function and this one is already odd, it follows that

$$\text{Im}[D_\alpha(\omega)] = m\gamma\omega\frac{\Lambda^2}{\omega^2+\Lambda^2}. \tag{2.3.10}$$

For the real part we calculate the Cauchy principal value of the following integral, separate the roots in the denominator and apply the residue theorem to study the poles on the upper semi-plane of the complex plane of ω'.

$$Re[D_\alpha(\omega)] = \frac{1}{\pi}m\gamma \quad P\int_{-\infty}^\infty d\omega'\frac{\omega'\Lambda^2}{(\omega'-\omega)(\omega'-i\Lambda)(\omega'+i\Lambda)}. \tag{2.3.11}$$

As the numerator has no poles we only need to care about the roots of the denominator. In figure 2.2 we can see the path used for the integral.

By virtue of the residue theorem we can split the corresponding path integral in the following manner:

$$\int_C f(\omega')d\omega' = \lim_{\epsilon\to 0}\left(\int_{-R}^{\omega-\epsilon}f(\omega')d\omega' + \int_{\omega+\epsilon}^R f(\omega')d\omega'\right) + \lim_{\epsilon\to 0}\int_{\omega-\epsilon,C_2}^{\omega+\epsilon}f(\omega')d\omega' + \int_{R,C_4}^{-R}f(\omega')d\omega'$$

$$= 2\pi i\sum_{a_i\in C}Res(f(\omega'),a_i) = 2\pi i\lim_{\omega'\to i\Lambda}(\omega'-i\Lambda)f(\omega'). \tag{2.3.12}$$

Where $f(\omega')$ is the integrand in 2.3.11 and we have made use of the residue theorem and the residue for a simple pole on the last line. Rearranging the terms in the last two lines and applying the limit $R\to\infty$ we can now solve 2.3.11.
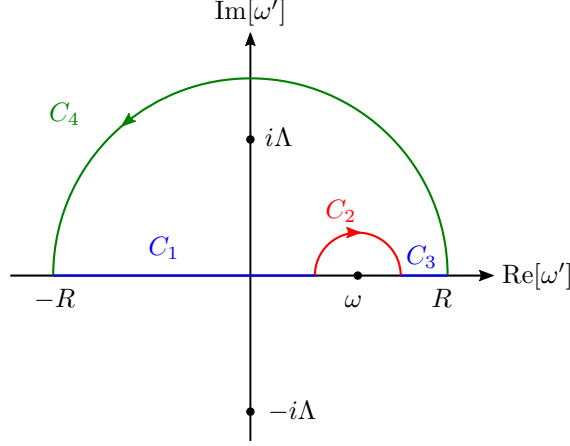
Figure 2.2: Diagram in the complex plane of ω' with the full path used for the real part integral of the susceptibility of an ohmic spectral density with a Drude Lorentz cut-off. The path C_2 is a semi circle centred on the pole $\omega' = \omega$ and has a radius $\epsilon \to 0$ made to avoid the singularity on the real axis and to join C_1, C_3 together. The other poles $\omega = i\Lambda, -i\Lambda$ present in the imaginary axis are represented as well.

$$Re[D(\omega)] = 2\pi i \lim_{\omega' \to i\Lambda} (\omega' - i\Lambda) f(\omega') - \lim_{\epsilon \to 0} \int_{\omega-\epsilon, C_2}^{\omega+\epsilon} f(\omega') d\omega' - \lim_{R \to \infty} \int_{R, C_4}^{-R} f(\omega') d\omega'. \tag{2.3.13}$$

The first term is a direct calculation by applying the imposed limit so that:

$$2\pi i \lim_{\omega' \to i\Lambda} (\omega' - i\Lambda) f(\omega') = m\gamma \frac{\Lambda^2}{\omega^2 + \Lambda^2} (\Lambda - i\omega). \tag{2.3.14}$$

For the second term in 2.3.13 we again use the residue theorem for a counter clockwise circle path around the pole in $\omega' = \omega$ and taking into account the direction of C_3 being the opposite and half of this path, we can write:

$$\lim_{\epsilon \to 0} \int_{\omega-\epsilon, C_2}^{\omega+\epsilon} f(\omega') d\omega' = -\pi i \sum Res(f(\omega')) = -m\gamma \frac{\Lambda^2}{\omega^2 + \Lambda^2} i\omega. \tag{2.3.15}$$

For the last term we take into account the estimation lemma [17] to show that the upper bound of the integral vanishes when $R \to \infty$.

$$\left| \lim_{R \to \infty} \int_{R, C_4}^{-R} f(\omega') d\omega' \right| \le Ml(C_4) = \lim_{R \to \infty} \frac{R}{(R - \omega)(R^2 - \Lambda^2)} \pi R = \lim_{R \to \infty} \frac{2\pi}{6R - 2\omega} = 0 \tag{2.3.16}$$

where we have used the triangle inequality to obtain M and the L'Hopital's rule to reduce the limit expression. M is the maximum value of the integrand and $l(C_4)$ is the arc length of the contour C_4. Introducing this results in 2.3.13:

15

$$Re[D(\omega)] = m\gamma \frac{\Lambda^2}{\omega^2 + \Lambda^2}\Lambda. \tag{2.3.17}$$

Finally, the susceptibility for this spectral density becomes:

$$D_\alpha(\omega) = m\gamma \frac{\Lambda^2}{\omega^2 + \Lambda^2}(\Lambda + i\omega). \tag{2.3.18}$$

Step function cut-off

We now proceed to employ an ohmic spectral density with a simple step function as the cut-off, so calculations to obtain the susceptibility are much simpler. In this case we define the spectral density as

$$J_{SF}(\omega) = m\gamma\omega\Theta(\omega)\Theta(\Lambda - \omega). \tag{2.3.19}$$

We repeat the procedure for K_α using 2.3.3 to that

$$K_{SF} = \frac{2}{\pi}\int_0^\infty d\omega \frac{J_{SF}(\omega)}{\omega} = \frac{2}{\pi}m\gamma\int_0^\infty \Theta(\omega)\Theta(\Lambda - \omega)d\omega = \frac{2}{\pi}m\gamma\Lambda. \tag{2.3.20}$$

The imaginary part is again very simple to calculate

$$\text{Im}[D_\alpha(\omega)] = m\gamma\omega\left[\Theta(\omega)\Theta(\Lambda - \omega) + \Theta(-\omega)\Theta(\Lambda + \omega)\right]. \tag{2.3.21}$$

Notice how the first term is not zero when $\omega \in [0, \Lambda]$ while on the second is when $\omega \in [-\Lambda, 0]$. When can then rewrite the expression as

$$\text{Im}[D_\alpha(\omega)] = m\gamma\omega\Theta(\Lambda - \omega)\Theta(\Lambda + \omega). \tag{2.3.22}$$

To integrate the real part we have to be aware of the restriction imposed by the principal value of the Cauchy integral, so that we have to separate in two cases due to the step function cut off. That is, first we integrate assuming $|\Lambda| > |\omega|$ and then for $|\Lambda| \leq |\omega|$.

For $|\Lambda| > |\omega|$:

$$\begin{aligned}
Re[D_\alpha(\omega)] &= \frac{1}{\pi}P\int_{-\infty}^{\infty} d\omega' m\gamma \frac{\omega'}{\omega' - \omega}\Theta(\Lambda - \omega')\Theta(\Lambda + \omega') \\
&= \frac{1}{\pi}\lim_{\epsilon \to 0}\left(\int_{-\Lambda}^{\omega-\epsilon} d\omega' m\gamma \frac{\omega'}{\omega' - \omega} + \int_{\omega+\epsilon}^{\Lambda} d\omega' m\gamma \frac{\omega'}{\omega' - \omega}\right) \\
&= \frac{1}{\pi}\lim_{\epsilon \to 0}\left(\int_{-\Lambda}^{\omega-\epsilon} d\omega' m\gamma \left(1 + \frac{\omega}{\omega' - \omega}\right) + \int_{\omega+\epsilon}^{\Lambda} d\omega' m\gamma \left(1 + \frac{\omega}{\omega' - \omega}\right)\right) \\
&= \frac{1}{\pi}\int_{-\Lambda}^{\Lambda} d\omega' m\gamma \left(1 + \frac{\omega}{\omega' - \omega}\right) - \lim_{\epsilon \to 0}\frac{1}{\pi}\int_{\omega-\epsilon}^{\omega+\epsilon} d\omega' m\gamma \left(1 + \frac{\omega}{\omega' - \omega}\right) \\
&= \frac{1}{\pi}m\gamma \left(2\Lambda + \omega\ln\left|\frac{\Lambda - \omega}{\Lambda + \omega}\right|\right). \tag{2.3.23}
\end{aligned}$$

Notice that in order to simplify the calculation we have used the fact that $\int_a^b f(x)dx + \int_c^d f(x)dx = \int_a^d f(x)dx - \int_b^c f(x)dx \ \forall f(x), a < b < c < d$.

For $|\Lambda| \leq |\omega|$:

$$Re[D_\alpha(\omega)] = \frac{1}{\pi} P \int_{-\infty}^{\infty} d\omega' m\gamma \frac{\omega'}{\omega' - \omega} \Theta(\Lambda - \omega')\Theta(\Lambda + \omega')$$

$$= \frac{1}{\pi} \lim_{\epsilon \to 0} \left(\int_{-\infty}^{\omega - \epsilon} d\omega' m\gamma \frac{\omega'}{\omega' - \omega} \Theta(\Lambda - \omega')\Theta(\Lambda + \omega') \right.$$

$$\left. + \int_{\omega+\epsilon}^{\infty} d\omega' m\gamma \frac{\omega'}{\omega' - \omega} \Theta(\Lambda - \omega')\Theta(\Lambda + \omega') \right). \qquad (2.3.24)$$

If we assume that ϵ is very small and for example $\omega \leq -|\Lambda|$ then the first integral vanishes with the step function and from the second one only the interval $[-\Lambda, \Lambda]$ survives, recovering the previous result for $|\Lambda| > |\omega|$. The opposite case of $\omega \geq |\Lambda|$ gives the same result.

Then, the susceptibility in this case is

$$D_{SF}(\omega) = \frac{1}{\pi} m\gamma \left(2\Lambda + \omega \ln \left| \frac{\Lambda - \omega}{\Lambda + \omega} \right| \right) + im\gamma\omega\Theta(\Lambda - \omega)\Theta(\Lambda + \omega). \qquad (2.3.25)$$

Super Ohmic with step function cut-off

Now we explore a similar model to the previous one albeit with the premise that it is super-ohmic; the spectral density does not depend linearly with ω but with a higher power. In this case we will study ω^2 but the analysis is similar to other values of s in ω^s.

The spectral density in this case will be defined as:

$$J_{SF}(\omega) = m\gamma \frac{\omega^2}{\Lambda} \Theta(\omega)\Theta(\Lambda - \omega). \qquad (2.3.26)$$

where the Λ as been added in the denominator for dimensional reasons.

K_α is calculated as

$$K_{SO} = \frac{2}{\pi} \int_0^{\infty} d\omega \frac{J_{SO}(\omega)}{\omega} = \frac{2}{\pi\Lambda} m\gamma \int_0^{\infty} \omega\Theta(\omega)\Theta(\Lambda - \omega)d\omega = \frac{m\gamma\Lambda}{\pi}. \qquad (2.3.27)$$

The imaginary part of the susceptibility is

$$Im[D_\alpha(\omega)] = m\gamma \frac{\omega^2}{\Lambda} \left[\Theta(\omega)\Theta(\Lambda - \omega) - \Theta(-\omega)\Theta(\Lambda + \omega) \right]. \qquad (2.3.28)$$

While the real part is computed in the same manner as in the last case, where $|\Lambda| \leq |\omega|$ will give the same result than $|\Lambda| > |\omega|$ due to the step function limit so we only compute the integral for the former case.

$$Re[D_\alpha(\omega)] = \frac{1}{\pi} P \int_{-\infty}^{\infty} d\omega' \frac{m\gamma}{\Lambda} \frac{\omega'^2}{\omega' - \omega} \left[\Theta(\omega')\Theta(\Lambda - \omega') - \Theta(-\omega')\Theta(\Lambda + \omega') \right]$$

$$= \frac{m\gamma}{\pi\Lambda} \left(\int_{-\Lambda}^{\Lambda} d\omega' \frac{\omega'^2}{\omega' - \omega} - \lim_{\epsilon \to 0} \int_{\omega-\epsilon}^{\omega+\epsilon} d\omega' \frac{\omega'^2}{\omega' - \omega} \right)$$

$$= \frac{m\gamma}{\pi\Lambda} \left(\int_{-\Lambda+\omega}^{\Lambda+\omega} d\omega'' \left(-\omega'' + \frac{\omega^2}{\omega''} + 2\omega \right) - \lim_{\epsilon \to 0} \int_{\omega-\epsilon}^{\omega+\epsilon} d\omega'' \left(\omega'' + \frac{\omega^2}{\omega''} + 2\omega \right) \right)$$

$$= \frac{m\gamma}{\pi\Lambda} \left(\Lambda^2 + \omega^2 \ln \left| \frac{\omega^2 - \Lambda^2}{\omega^2} \right| \right). \qquad (2.3.29)$$

Then, the susceptibility in this case is

$$D_{SO}(\omega) = \frac{m\gamma}{\pi\Lambda}\left(\omega^2\ln\left|\frac{\omega^2-\Lambda^2}{\omega^2}\right|+\Lambda^2\right)+im\gamma\frac{\omega^2}{\Lambda}\left[\Theta(\omega)\Theta(\Lambda-\omega)-\Theta(-\omega)\Theta(\Lambda+\omega)\right].$$
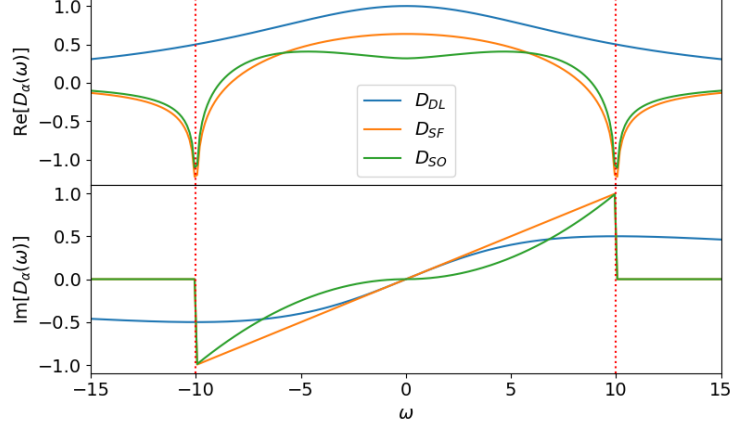
(2.3.30)

Figure 2.3: Real (upper) and imaginary (lower) parts of the susceptibilities under study. D_{DL} is ohmic with Drude Lorentz term, D_{SF} is ohmic with a step function cut off and D_{SO} is super ohmic with a step function cut off. The vertical dotted line marks the cut off $\omega = \pm\Lambda$. $\Lambda = 10, \gamma = 0.1, m = 1$.

In figure 2.3 we can see some differences and similarities between the models. For the susceptibilities controlled by the step function cut off, their behaviour is almost identical outside $\omega \in [-\Lambda, \Lambda]$ but inside we can see some differences. In the imaginary part of $D_\alpha(\omega)$ the linear profile of the ohmic model is contrasted with the quadratic profile of the super ohmic one. In the real part, the super ohmic model exhibits two maximum points, whereas the ohmic models only have one.

Similarly, we can see the differences between the two ohmic models. In both the imaginary and real parts of $D_\alpha(\omega)$ the Drude Lorentz model is modulated by the Lorentzian while the step function model shows a discontinuity at $\omega = \pm\Lambda$. Also notice that $\mathrm{Re}[D_\alpha(\omega)] \geq 0, \forall\omega$ for the Drude Lorentz model.

Chapter 3

Applications of the model

In this chapter we will begin by illustrating the theory with some simple scenarios that exemplify the properties of this model and we will advance onto larger pictures with an special interest in the analysis of heat currents and temperature profiles.

3.1 One oscillator on a Caldeira-Legget bath

This simple scheme was one of the first approaches to describe a Brownian particle under the quantum regime and is relevant in our study as a way to portrait in a simpler way the influence of the spectral density in the behaviour of the system. It also serves to compare the model to the thermal state result, which gives us a way to measure the thermalisation of the system by means of the elements in the covariance matrix. Although this case is easy to obtain on it's own, we will simply particularise the equations found previously for the case of one oscillator and one Caldeira-Legget bath.

The general Hamiltonian described at the beginning of chapter 2 can be specified for this scenario as

$$\hat{H}_S = \frac{\hat{p}^2}{2m} + \frac{1}{2}m\Omega^2\hat{x}^2, \tag{3.1.1}$$

$$\hat{H}_B = \sum_{\mu} \frac{\hat{p}_{\mu}^2}{2m_{\mu}} + \frac{1}{2}m_{\mu}\omega_{\mu}^2\hat{x}_{\mu}^2, \tag{3.1.2}$$

$$\hat{H}_{SB} = \hat{x}\sum_{\mu} g_{\mu}\hat{x}_{\mu}. \tag{3.1.3}$$

The Hamiltonian $\hat{H}_S$ defines the kinetic and potential energy of the oscillator, $\hat{H}_B$ accounts for all the oscillators in the bath and $\hat{H}_{SB}$ describes the interaction between the oscillator and the bath. The renormalised frequency is obtained by $\Omega^2 = \omega_0^2 + \frac{K}{m}$ and the temperature of the bath will be T.

3.1.1 Covariance Matrix

Specifying (2.2.22) for only one oscillator yields:

$$\hat{X}(\omega) = A(\omega)\hat{F}(\omega) = \frac{1}{m(\Omega^2 - \omega^2) - D(\omega)}\hat{F}(\omega). \tag{3.1.4}$$

Particularising (2.2.30-2.2.33) will result in the following terms

$$\sigma_{xx} = \frac{\hbar}{2\pi} \int_{-\infty}^{\infty} d\omega A(\omega) A(-\omega) \coth\left(\frac{\hbar\omega}{2K_B T}\right) \text{Im}[D(\omega)], \qquad (3.1.5)$$

$$\sigma_{pp} = \frac{\hbar}{2\pi} m^2 \int_{-\infty}^{\infty} d\omega \omega^2 A(\omega) A(-\omega) \coth\left(\frac{\hbar\omega}{2K_B T}\right) \text{Im}[D(\omega)], \qquad (3.1.6)$$

and $\sigma_{xp} = \sigma_{px} = 0$ as seen in equation 2.2.34. For the numerical calculations the script used is written in Python and relies on `scipy.integrate.quad` method to obtain the desired integral. This method is specially designed to compute improper integrals by adjusting the integration step whenever needed up to a certain imposed limit in order to make a more efficient integration. For more information on the method please refer to the Fortran QUADPACK library.

We now compare the evolution of this system for different spectral densities at different temperatures as well as different values of γ. We will also introduce an harmonic oscillator in a thermal state with covariance matrix:

$$\sigma_{xx} = \frac{\hbar}{2m\omega_0} \coth\left(\frac{\omega_0 \hbar}{2K_B T}\right), \qquad (3.1.7)$$

$$\sigma_{pp} = \frac{\hbar m\omega_0}{2} \coth\left(\frac{\omega_0 \hbar}{2K_B T}\right), \qquad (3.1.8)$$

$$\sigma_{xp} = \sigma_{px} = 0. \qquad (3.1.9)$$

In the following analysis as well as in the rest of this work we will assume $m_i = k_B = \hbar = 1$ for the sake of simplicity.
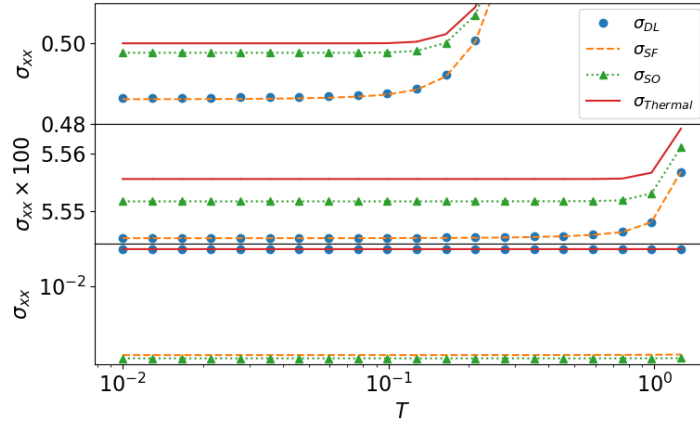

Figure 3.1: Evolution of σ_{xx} in a system of one oscillator with temperature of the bath T in Log-Log scale. This is done for different models of spectral density: DL stands for ohmic spectral density with a Drude Lorentz cut off, SF for ohmic with step function cut off and SO for super ohmic with step function cut off. They are also compared with the thermal state. Different values of ω_0 are used to compare its relative value with Λ: $\omega_0 = 1$ (upper), $\omega_0 = 9$ (middle) and $\omega_0 = 11$ (lower). The middle graph y-axis is scaled by a $\times 100$ factor for readability. $\Lambda = 10$, $\gamma = 0.1$.

As one can see in figures 3.1, 3.2 the super ohmic bath seems to follow the thermal equilibrium of a harmonic oscillator better than the ohmic ones, although at greater temperatures the profiles converge. However, when the natural frequency ω_0 is outside of the
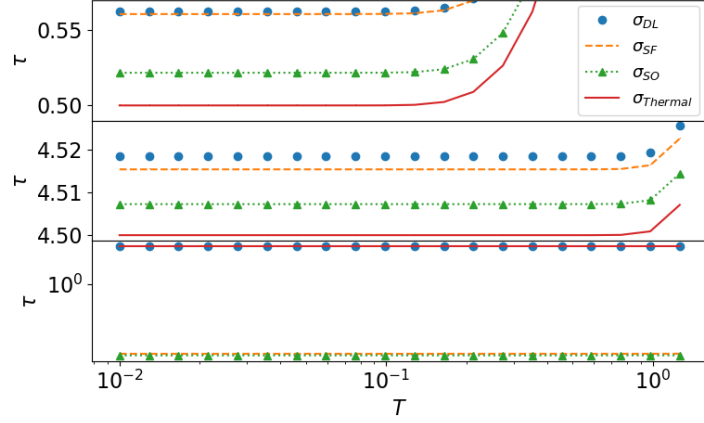
Figure 3.2: Evolution of τ in a system of one oscillator with temperature of the bath T in Log-Log scale. Same parameters and conditions as in figure 3.1.

cut off Λ, the ohmic model with a Drude Lorentz cut off is in a better agreement than the ones based on a step function. This makes sense as the Drude Lorentz term allows for exploration of higher frequency values than Λ. Thus a non linear model with a continuous decay seems to be the most accurate model to work with, albeit it might not be as simple as the ones showcased.

It is also interesting to see that the point where the kinetic temperature of the oscillator starts to agree with the temperature of the bath shifts with ω_0 in figure 3.2. At low temperatures the harmonic potential is stronger than the kinetic energy provided by the bath so the oscillator stays on it's natural frequency. When the temperature increases with respect to ω_0, the interaction with the bath starts to gain importance in the energy balance and the temperature of the oscillator begins to get closer to that of the bath.

3.2 Chain of two oscillators and two baths

This simple case is useful to study first and foremost the interaction between two oscillators connected through a coupling, which can be a sufficiently interesting system to study for example the effects of thermal probing at very low temperatures [18].

We start by considering the Hamiltonian of a system of two oscillators connected to each other by a harmonic coupling of strength k and each of them connected to a different Caldeira-Legget bath at temperatures T_L, T_R.

$$\hat{H}_S = \sum_{i=1,2} \frac{\hat{p}_i^2}{2m_i} + \frac{1}{2}(m_i\omega_{0,i}^2 + \sum_{\alpha=L,R} c_{i,\alpha}^2 K_\alpha + k)\hat{x}_i^2 - k\hat{x}_1\hat{x}_2, \qquad (3.2.1)$$

$$\hat{H}_B = \sum_{\alpha=L,R} \sum_{\mu_\alpha} \frac{\hat{p}_{\mu_\alpha}^2}{2m_{\mu_\alpha}} + \frac{1}{2m_{\mu_\alpha}}\omega_{\mu_\alpha}^2 \hat{x}_{\mu_\alpha}^2, \qquad (3.2.2)$$

$$\hat{H}_{SB} = \sum_{i=1,2} \hat{x}_i \sum_{\alpha=L,R} c_{i,\alpha} \sum_{\mu_\alpha} g_{\mu_\alpha} \hat{x}_{\mu_\alpha}, \qquad (3.2.3)$$

with $c_{1,L} = 1$, $c_{1,R} = 0$, $c_{2,L} = 0$, $c_{2,R} = 1$.

3.2.1 Covariance Matrix

The full covariance matrix at the steady state for N=2 takes the form:

$$\sigma = \begin{bmatrix} \sigma_{x_1,x_1} & \sigma_{x_1,p_1} & \sigma_{x_1,x_2} & \sigma_{x_1,p_2} \\ \sigma_{p_1,x_1} & \sigma_{p_1,p_1} & \sigma_{p_1,x_2} & \sigma_{p_1,p_2} \\ \sigma_{x_2,x_1} & \sigma_{x_2,p_1} & \sigma_{x_2,x_2} & \sigma_{x_2,p_2} \\ \sigma_{p_2,x_1} & \sigma_{p_2,p_1} & \sigma_{p_2,x_2} & \sigma_{p_2,p_2} \end{bmatrix}. \tag{3.2.4}$$

As an illustration, we show the result for the elements σ_{x_i,p_j} which are a specific case of 2.2.31.

$$\sigma_{x_i,p_j} = \frac{i\hbar}{2\pi} m_j \int_{-\infty}^{\infty} d\omega \omega \Big[A_{i1}(\omega) A_{j1}(-\omega) \coth\left(\frac{\hbar\omega}{2K_B T_L}\right) \mathrm{Im}[D_L(\omega)]$$
$$+ A_{i2}(\omega) A_{j2}(-\omega) \coth\left(\frac{\hbar\omega}{2K_B T_R}\right) \mathrm{Im}[D_R(\omega)] \Big]. \tag{3.2.5}$$

3.2.2 Heat Current

For this scenario we specify (2.2.44) for 2 oscillators, Thus in the steady state:

$$\dot{Q}_\alpha = -\sum_i c_{i,\alpha} \frac{1}{m_i} k \sigma_{p_i,x_j}|_{j\neq i}. \tag{3.2.6}$$

For low values of the coupling between oscillators and high bath temperatures one would expect the oscillators to behave as isolated systems, which is precisely what we see in figure 3.3. It can be argued that the influence of the baths is more relevant than the coupling in such a scenario. Of course, when we increase the coupling the oscillators tend to find a group temperature. The same argument can be used for the case of lower temperatures, since the coupling influence is more comparable with the interaction with the baths. Notice how the heat currents stay balanced across all values of k, since the energy is transmitted from one oscillator onto the other and there are no sources that could perturb this balance.

It can be perceived that, as seen previously in figure 3.2, the temperature of the oscillators slightly differ from the temperature of the baths for small k in figure 3.3, where this discrepancy can be modulated with γ. At slightly higher values of k the kinetic temperature of the oscillators start to go to an average as the coupling is intense enough to allow for heat transfer, as can be seen in the evolution of $\dot{Q}$ with k. At even higher values of k the definition of kinetic temperature doesn't hold the same meaning as the harmonic coupling now dominates the heat transfer process.

In figure 3.4 we see how the currents for this model might be affected by different spectral density models. Two different regimes are shown, low temperatures and high temperatures. For this particular combination of parameters the heat current of the super ohmic model is smaller than the ohmic one for low temperatures but the opposite happens at high temperatures. This is not always the case, as the parameters play an important role in this relative growth. At low temperatures the heat current in all models evolve in a non linear profile which is heavily dependent on the combination of spectral density, k and γ as seen in appendix C. At high temperatures the current in all models grows linearly with ΔT. Please notice that we are talking about the logarithmic scale as the growth is actually exponential.

3.3 Comparison with Classical Scenario

One relevant way to test this calculations is to also deduce the expressions for a classical chain of oscillators with the same constrains. The Hamiltonian is basically identical except for the
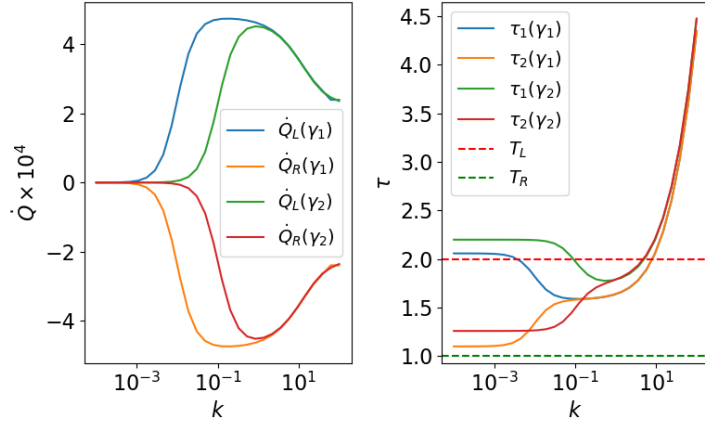
Figure 3.3: Evolution of a two oscillator system with the linear coupling k, each oscillator connected to one bath of temperatures $T_L = 2, T_R = 1$, red and green dashed lines respectively. Both baths have the same spectral density and coupling factor γ to the oscillators. Left graph represents the heat currents associated with each bath and the right graph indicates the oscillator temperature τ_i. The heat current has being increased by a factor of 10^4 for readability. $\Lambda = 10, \gamma_1 = 10^{-2}, \gamma_2 = 10^{-1}, m_i = 1$.
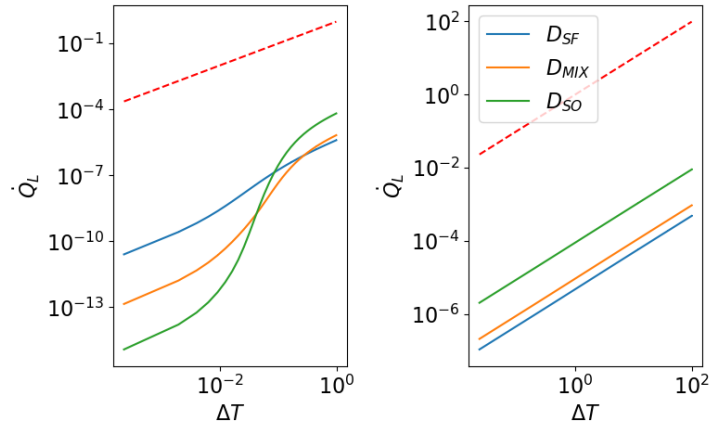

Figure 3.4: Evolution of the heat current of the left bath with the difference in temperature between baths for a two oscillator model. Three spectral density cases have been employed. Ohmic spectral density with step function cut off (blue), super ohmic spectral density with step function cut off (green) and a mix with the left bath as ohmic and the right as superohmic, both with step function cut off (orange). The red line represents $\dot{Q} = \Delta T$ in order to reflect the asymptotic behaviour of the currents in the double logarithmic scale. For the left graph: $T_R = 0.01$. For the right graph $T_R = 1$. $\Lambda = 10, \gamma = 10, m_i = 1, k = 10^{-2}$.

use of coordinates instead of operators. We follow the same procedure of renormalisation as well.

$$H_S = \sum_{i=1}^{N} \frac{p_i^2}{2m_i} + \frac{1}{2}m_i\Omega_i^2 x_i^2 + -k_{i,i+1}x_i x_{i+1} + \frac{1}{2}\sum_{i=1}^{N}\sum_{j=1,j\neq i}^{N} K_{ij}x_i x_j, \qquad (3.3.1)$$

$$H_B = \sum_{\alpha} H_{B,\alpha} = \sum_{\alpha}\sum_{\mu_\alpha} \frac{p_{\mu_\alpha}^2}{2m_{\mu_\alpha}} + \frac{1}{2}m_{\mu_\alpha}\omega_{\mu_\alpha}^2 x_{\mu_\alpha}^2, \qquad (3.3.2)$$

$$H_{SB} = \sum_{i=1}^{N} x_i \sum_{\alpha} c_{i,\alpha} B_\alpha = \sum_{i=1}^{N} x_i \sum_{\alpha} c_{i,\alpha} \sum_{\mu_\alpha} g_{\mu_\alpha} x_{\mu_\alpha}. \qquad (3.3.3)$$

We can obtain the results of Hamilton's equations ($\dot{q} = \frac{dH}{dp}$; $\dot{p} = -\frac{dH}{dq}$) which are the equivalent to the equations of motion obtained through $\frac{d\hat{O}}{dt} = \frac{i}{\hbar}[\hat{H}, \hat{O}]$. It is of no surprise that this yield the same results as previous calculations with the commutators.

$$m_i\ddot{x}_i(t) = -m_i\Omega_i^2 x_i(t) + k_{i,i+1}x_{i+1}(t) + k_{i-1,i}x_{i-1}(t),$$
$$-\sum_{j=1,j\neq i}^{N} K_{ij}x_j(t) + \sum_{\alpha} c_{i,\alpha}\left(f_\alpha(t) + \sum_{k=1}^{N} c_{k,\alpha}d_\alpha(t)*x_k(t)\right). \qquad (3.3.4)$$

Thus we can follow the same procedures as before in order to simplify the equations and the only difference left is the classical fluctuation dissipation relation (see Appendix A).

$$\frac{1}{2}\langle\{F_\alpha(\omega), F_\alpha(\omega')\}\rangle = \delta(\omega+\omega')\left(\frac{4\pi K_B T}{\omega}\right)\text{Im}[D_\alpha(\omega)]. \qquad (3.3.5)$$

One can quickly notice that the expression resulting from this is a first order approximation of the quantum relation 2.2.28, except for the absence of the Plank constant, since performing a Taylor expansion yields $\coth(x) = \frac{1}{x} + \frac{x}{3} - \frac{x^3}{45} + [\ldots]$. Notice that the argument in the coth is inversely proportional to the temperature of the bath, so the terms of second order decrease with T. It is safe to assume then that the classical representation will yield the same result as the quantum counterpart when the temperature increases. The friction parameter γ defines the spectral density and affects the convergence rate with temperature, albeit modestly. The influence of this parameter is difficult to study analytically due to the inverse matrix calculation but assuming γ is sufficiently large in comparison to $m_i, k_{i,i+1}$ it will dominate 2.2.22, as one can see in figure 3.5. Thus, the product $A_{ik}(\omega)A_{jl}(-\omega)$ present in the covariance matrix elements will be dominated by $\frac{1}{\gamma^2}$. On the other hand, $\text{Im}[D_\alpha(\omega)] \propto \gamma$ so at the end the factor $\frac{1}{\gamma}$ will influence the result. This matches the classical result were a T/γ ratio defines the behaviour of the system, but in the quantum picture is also influenced by higher order terms: $\frac{1}{\gamma T}, \frac{1}{\gamma T^3}, \ldots$. Since T is low at the quantum regime, this terms are more relevant than $\frac{T}{\gamma}$ and thus the behaviour is not so intuitive.

However, if we fix the temperatures on two baths and increase one of them, an interesting phenomena arises from the difference between the classic and quantum pictures. As we can see in figure 3.6 the difference between the models is heavily dependant on γ as it saturates to a fixed difference for a particular value of this parameter for the oscillator in the bath which increases in temperature. Here the dependence with γ is more interesting as the difference in the models reaches an asymptotic value, dependant on γ, sooner for small γ and later for bigger values of this parameter. When the difference in temperature of the oscillators becomes too big, the quantum model fails to replicate the results of the classic one, but for small differences in temperature the evolution is very similar to figure 3.5.
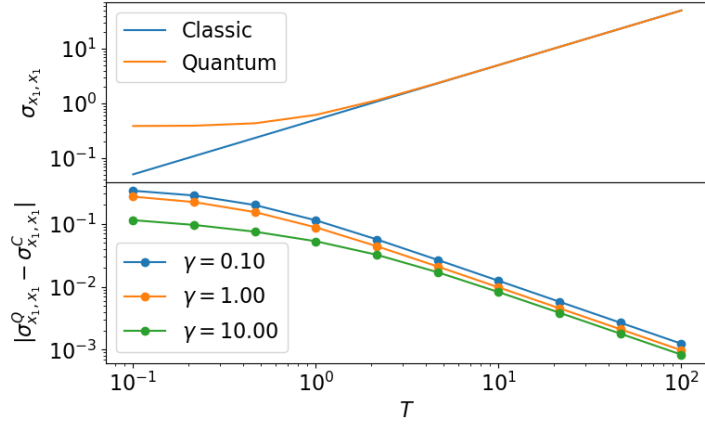
Figure 3.5: Convergence of the classic and quantum results for the covariance matrix element σ_{x_1,x_1} for a 2 bath model of 1 oscillator each, where the temperature is increased for all baths. $T_L = T, T_R = \frac{T}{2}$. The upper graph represents this three evaluations at different T with $\gamma = 0.1$, The lower graph indicates the difference between the quantum model (denoted with upper index Q) and the classical model (denoted with upper index C) for different values of γ. The spectral density used was ohmic with Drude Lorentz cut off. $m = 1, \omega_0 = 1, \Lambda = 10, \gamma_0 = 0.1$
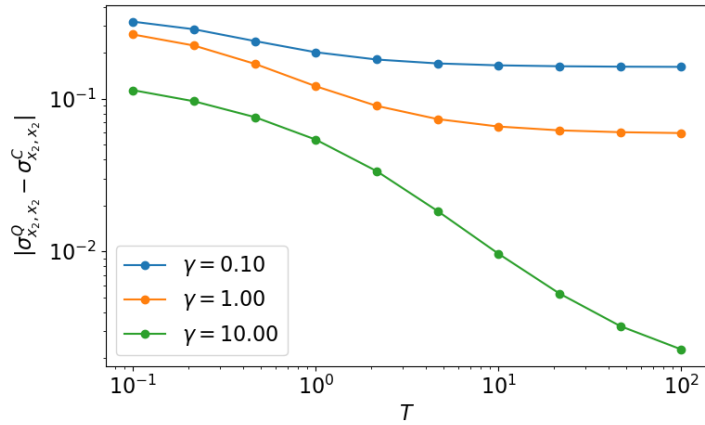

Figure 3.6: Comparison of the classic and quantum results for the covariance matrix element σ_{x_2,x_2} for a 2 bath model of 1 oscillator each, where the temperature is increased for only one bath. $T_L = 10^{-1}, T_R = \frac{T}{2}$. The graph indicates the difference between the quantum model (denoted with upper index Q) and the classical model (denoted with upper index C) for different values of γ. The spectral density used was ohmic with Drude Lorentz cut off. $m = 1, \omega_0 = 1, \Lambda = 10, \gamma_0 = 0.1$

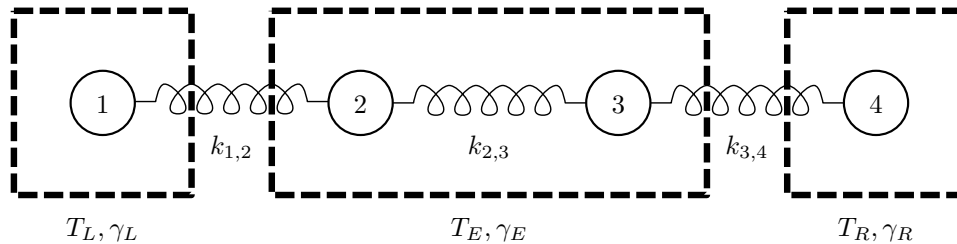## 3.4 Chain of four oscillators and three baths

Figure 3.7: Schematic for a chain of four linearly coupled oscillators. The circles represent the oscillators. The springs represent the linear harmonic coupling between first neighbours. The dashed line boxes represent the baths and their interaction with the oscillators on their interior. Temperature and coupling labels are assigned for each bath as well as to each pair of coupled oscillators.

As portrayed in figure 3.7 we now study a chain of four oscillators distributed in three baths: left (L), intermediate or environment (E) and right (R). The left and right baths contain one oscillator each while the intermediate bath contains two. The aim of this section is to study the temperature profile of a chain where the bath E is not present and to measure the heat transfer though a system where the oscillators of bath E are not coupled. This will allow us to predict results for larger chains of similar characteristics.

3.4.1 Temperature profile

In this case the described model of four oscillators has the bath E removed, which can be done by assuming $\gamma_E = 0$. This can be understood as if the oscillators in the intermediate bath stand in a very low interactive environment, being only influenced by the other oscillators in the chain. All the oscillators will be connected to their first neighbours. We want to compare such a scenario with the already explained two oscillator system, and to review the temperature profile of both models under similar conditions. In principle one would expect to see the oscillators in between baths to act as an effective coupling, but the interactions might prove to be no so trivial.

In figure 3.8 we can observe a slight difference in the temperature profiles between the two models proposed. The ohmic case shows a higher kinetic temperature in τ_1 than the one provided by T_L, τ_2, τ_3 are balanced and τ_4 is slightly higher than T_R. This is expected from the findings in figure 3.3 but the super ohmic model shows a more linear profile, where τ_1 is lower than T_L, τ_2, τ_3 have different values and τ_4 is even higher than in the case of the ohmic baths. One could assume this is due to the definition of kinetic temperature used. However, as seen in the two oscillator scheme, the bath model affects the evolution of the heat current with temperature so it is more reasonable to assume the bath models are entirely responsible for this difference between the profiles.

3.4.2 Broken chain

In this case we study the chain of four oscillators with three baths present where the chain has a broken link in its middle, so that $k_{2,3} = 0$. We use the coupling of the oscillators with the middle bath, γ_E, as our parameter.

This proposal seeks to observe how the heat currents of the baths are affected by a broken link between intermediate oscillators in the bath, as breaking the coupling between oscillators of different baths would give the trivial result of the absence of energy transfer
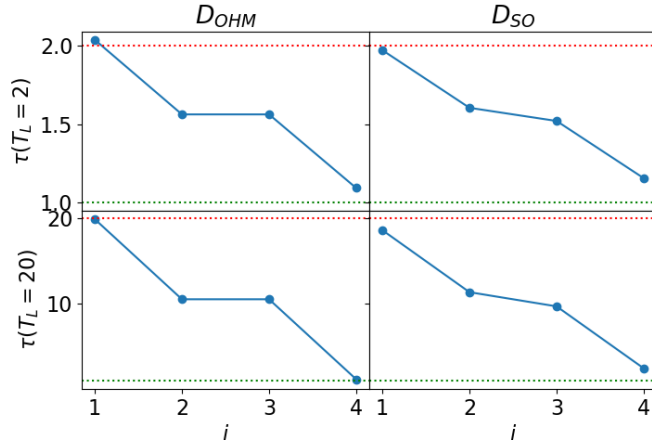
Figure 3.8: Temperature profile of the oscillators in a model of $N = 4$ oscillators where $N_L = N_R = 1$. Each column represents one spectral density model combination. From left to right: ohmic-ohmic, super ohmic-super ohmic. Each row uses a different temperature for the left bath. The temperature of the left bath (red dotted line) and the right bath (green dotted line) are shown for each case. $T_R = 1, k = 10^{-3}, \gamma_L = \gamma_R = 10^{-2}, \Lambda = 10$. $\omega_i = 1$.

between them. However, this case is not so simple since even if the coupling is non existent the oscillators might be able to communicate energy through the bath itself.

We can observe that in the case of $T_E = T_R$ we have a non-zero value for $\dot{Q}_R$ in the ohmic case when γ_E is small as seen in figure 3.9. Notice how the value becomes small very fast with γ_E. This implies an exchange of heat from baths L to R through the bath E and not from the coupling, since it has been severed at the middle of the chain. But only at $\gamma_E \ll 1$, for large values of this parameter the chain behaves as if the bath E contributes less and less to the heat transfer and the heat passes from bath L to bath R.
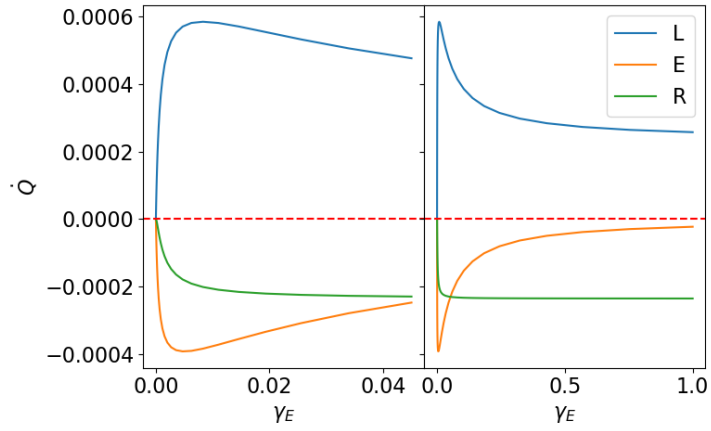
Figure 3.9: Heat current of each bath in an oscillator chain with respect to the coupling parameter γ_E. The chain has three baths (L,E,R) and a length of $N = 4$. The link between the second and third oscillator is broken ($k_{2,3} = 0$). The system exhibits a temperature profile of $T_L = 2, T_E = 1, T_R = 1$. The left graph shows the obtained values at a short range of γ_E while the right graph shows a longer range. The spectral density used is ohmic with a step function cut off. A horizontal red dashed line at $\dot{Q} = 0$ is draw as reference. $\gamma_L = \gamma_R = 0.1, k = 10^{-2}, \Lambda = 10$.

Chapter 4

Conclusions

In this work we have studied open quantum systems by means of a system plus reservoir method using the Caldeira-Legget model in order to obtain analytical solutions for a harmonic chain of oscillators at the steady state. From there on valuable tools such as the heat current and the kinetic temperature of the oscillators were established and reviewed. A brief look into spectral densities gave an insight into the importance of the form of interaction between the bath and the chain oscillators.

Different scenarios were explored, starting from the simplest case of one oscillator and one bath up until removing specific pair couplings in a small chain of oscillators. A comparison with the classical result was explored as well to see if the quantum model is effectively coherent with temperatures associated with the nanoscopic scale. We also validated the classical result as a first order approximation of the presented result for the quantum regime.

Relevant results such as the energy transfer through the terms of the bath where obtained, opening possibilities for further work on interesting topological defects in order to modulate the interactions along larger chains of oscillators.

Possible extensions of this work range from increasing the size of the system under study to the use of non harmonic coupling or the analysis of the system outside of the steady state. This last proposal would require a different framework as the solutions in such a case are not analytical.Another interesting topic that would not require further theoretical development for the framework would be the use of more varied topological defects on larger chains, as discussed before, which might show interesting results in the heat currents of the system. However, this extension proves difficult until a proper integration method for the model under study is implemented. The integration of the terms of the covariance matrix is not trivial and the code used needs to be properly examined , as discussed in appendix C .

Chapter 5

Resumen en Español

Cuando se trata de estudiar un sistema cuántico grande y complejo resulta útil buscar variables dinámicas del sistema que lo describan por completo, ignorando sus constituyentes individuales. Sin embargo, cuando el interés recae en ciertos componentes particulares del mismo se hace necesario el análisis desde el estudio de sistemas cuánticos abiertos.

Históricamente han existido múltiples propuestas para resolver este problema, recayendo usualmente en dos categorías generales: cuantización canónica del sistema mediante condiciones de contorno específicas y el uso de modelos de sistema cerrado más sistemas abiertos en forma de baños. Los primeros tienen la ventaja de funcionar de forma muy eficiente dentro de sus condiciones de contorno, pero suelen violar principios cuánticos elementales como el principio de superposición. Por otra parte, los métodos de sistema más baño proporcionan una mirada mucho más intuitiva, con una canonización cuántica más directa pero que fallan en reproducir algunos fenómenos cuánticos particulares como el tuneleado cuántico.

Este trabajo se centrará en el método de sistema más baño. Específicamente en, a través de imagen de Heisenberg, obtener la ecuación de Langevin cuántica para dar un resultado exacto bajo régimen de estado estacionario, de forma que se podrá analizar el sistema de forma analítica. Para ello son necesarias algunas condiciones como el uso de osciladores armónicos en el sistema, acoples lineales entre elementos del sistema y también se asumirá un modelo unidimensional de cadena abierta.

Para los baños será utilizado el modelo de Caldeira-Legget, el cual es un modelo semi empírico donde el baño queda definido por un número infinito de osciladores armónicos independientes entre sí. Este es un modelo que posee la ventaja de representar mecanismos realistas a la par de ser analíticamente resoluble. El baño queda totalmente definido a través de la densidad espectral, cuya forma será atribuida en los modelos óhmicos y super óhmicos empleados.

Para obtener los resultados pertinentes, primeramente se buscará la ecuación cuántica de Langevin para un sistema general de cadena de osciladores armónicos. A partir del Hamiltoniano del sistema, previa renormalización necesaria debido a la influencia del baño en las posiciones de equilibrio de los osciladores, se desarrollarán las ecuaciones de movimiento y se identificarán los términos correspondientes en comparación con la ecuación clásica de Langevin. He ahí se obtiene la matriz de covarianza en el estado estacionario, que permite definir propiedades termodinámicas como la temperatura de los osciladores o las corrientes de calor en función de sus elementos de matriz.

Llegados a este punto, se hace necesario definir con mayor claridad la densidad espectral y a partir de ella la susceptibilidad. Se ejemplificarán y tratará el desarrollo de los modelos empleados en este trabajo: el modelo óhmico de Drude Lorentz, el modelo óhmico con función paso y el modelo super óhmico cuando $s = 2$ con función paso. Los resultados obtenidos con estos modelos serán comparados a lo largo del trabajo bajo distintas aplicaciones.

Con estas herramientas se comienza a trabajar en casos específicos para poner en valor

la teoría desarrollada así como para obtener resultados y conclusiones relevantes.

Primeramente se particularizan las ecuaciones obtenidas para el caso simple de un oscilador y un baño. En este punto se estudiará en detalle el límite de bajas temperaturas y la importancia de la elección del modelo de densidad espectral al comparar los resultados obtenidos con el estado térmico de un oscilador armónico. Se obtendrá una discrepancia entre la temperatura del baño y la temperatura cinética del oscilador en el régimen de bajas temperaturas, cuyo límite vendrá dado por la frecuencia natural del oscilador.

Se continuará con el caso de dos osciladores y dos baños, en el que se observará la evolución de la temperatura de los osciladores con el acoplamiento entre los osciladores de la cadena, así como con el acoplamiento con los baños. Seguidamente se comparará la corriente de calor con la temperatura. Se diferenciará entre distintas densidades espectrales y distintos acoplamientos entre baños y osciladores. A partir de los resultados obtenidos se podrá observar como la definición de temperatura cinética empleada no resulta fiable para el régimen de altas temperaturas. Para concluir el estudio de este caso, se compararán los valores obtenidos bajo la ecuación cuántica de Langevin con su análogo clásico y se analizará el comportamiento de los mismos con la temperatura. Se tratará de ver así la diferencia entre ambos modelos a altas temperaturas y revelar bajo qué condiciones están de acuerdo.

Se finalizará este trabajo resolviendo el caso de una cadena de cuatro osciladores con tres baños, donde los osciladores en los extremos de la cadena estarán conectados a un baño cada uno y los dos osciladores intermedios conectados a un tercer baño. De esta forma se hace posible observar comportamientos del modelo general propuesto bajo condiciones más complejas: la ausencia de un baño intermedio o la transferencia de calor a través de un baño en el que sus osciladores están desacoplados entre sí. Para el primer caso de ausencia de baño intermedio se procederá a observar el comportamiento del perfil de temperatura de los osciladores dependiendo del modelo de baño aplicado y a recabar conclusiones al respecto. Por otra parte, se estudiarán las corrientes de calor para el caso en el que el baño intermedio está efectivamente conectado a sus correspondientes osciladores pero estos se hayan desacoplados entre sí. Para poder interpretar correctamente el valor hallado de las corrientes se fijará la temperatura del baño intermedio como la de uno de los baños en los extremos y se observará la evolución de las corrientes con el acoplamiento al baño intermedio. Se obtendrá que además de haber corriente de calor, existe un valor no nulo en la corriente del baño intermedio, por lo que el baño también es responsable de la transferencia de calor, no solo lo es el acople entre osciladores.

Los resultados obtenidos abren pie a extensiones de este trabajo tales como el estudio de cadenas de osciladores de mayor tamaño, el uso de acoples no armónicos entre osciladores o el estudio del sistema fuera del régimen estacionario.

En los apéndices del trabajo se añaden algunos resultados necesarios para el desarrollo de la teoría, así como un corto análisis del procedimiento numérico utilizado.

Appendix A

Fluctuation-Dissipation Relation

The Fluctuation-Dissipation relation is classically defined as [19, 20]:

$$S_F(\omega) = \frac{1}{2}\langle\{F_\alpha(\omega), F_\alpha(\omega')\}\rangle = \delta(\omega + \omega')\frac{4\pi K_B T}{\omega}\mathrm{Im}[D_\alpha(\omega)]. \tag{A.0.1}$$

Although the Fluctuation-Dissipation Relation is well known for classical systems, this relation can also be established for particular quantum scenarios such as the one we are studying [20, 21]. Let us begin with $\frac{1}{2}\langle\{f_\alpha(t), f_\alpha(t')\}\rangle$. First we need to reduce the anti commutator, so

$$\frac{1}{2}\langle\{f_\alpha(t), f_\alpha(t')\}\rangle = \frac{1}{2}\langle f_\alpha(t)f_\alpha(t') + f_\alpha(t')f_\alpha(t)\rangle = \langle f_\alpha(t)f_\alpha(t')\rangle. \tag{A.0.2}$$

since (2.2.17) commutes.

The bosonic thermal occupation number is defined from $2n_{\mu_\alpha}(T) + 1 = \coth\left(\frac{\hbar\omega}{2K_B T}\right)$ so that

$$n_{\mu_\alpha}(T) = \frac{1}{e^{\frac{\hbar\omega}{K_B T}} - 1}. \tag{A.0.3}$$

Taking into account $n_{\mu_\alpha}(T)$ we can calculate the expected value for different products of the canonical coordinates at the initial state of the system.

$$\langle x_{\mu_\alpha}(t_0)x_{\mu'_\alpha}(t_0)\rangle = \delta_{\mu_\alpha\mu'_\alpha}\hbar\frac{1 + 2n_{\mu_\alpha}(T)}{2m_{\mu_\alpha}\omega_{\mu_\alpha}}, \tag{A.0.4}$$

$$\langle p_{\mu_\alpha}(t_0)p_{\mu'_\alpha}(t_0)\rangle = \delta_{\mu_\alpha\mu'_\alpha}\frac{\hbar}{2}m_{\mu_\alpha}\omega_{\mu_\alpha}[1 + 2n_{\mu_\alpha}(T)], \tag{A.0.5}$$

$$\langle x_{\mu_\alpha}(t_0)p_{\mu'_\alpha}(t_0)\rangle = \langle p_{\mu_\alpha}(t_0)x_{\mu'_\alpha}(t_0)\rangle^* = \delta_{\mu_\alpha\mu'_\alpha}\frac{i\hbar}{2}. \tag{A.0.6}$$

Then from 2.2.17 and 2.3.3:

$$\begin{aligned}
\frac{1}{2}\langle\{f_\alpha(t'), f_\alpha(t'')\}\rangle = &\frac{\hbar}{\pi}\sum_{\mu_\alpha}\frac{\pi g_{\mu_\alpha}^2}{2m_{\mu_\alpha}\omega_{\mu_\alpha}}[1 + 2n_{\mu_\alpha}(T)] \\
&\cdot [\cos\omega_{\mu_\alpha}(t' - t_0)\cos\omega_{\mu_\alpha}(t'' - t_0) + \sin\omega_{\mu_\alpha}(t' - t_0)\sin\omega_{\mu_\alpha}(t'' - t_0)] \\
= &\frac{\hbar}{\pi}\int_0^\infty d\omega J_\alpha(\omega)\coth\left(\frac{\hbar\omega}{2K_B T}\right)\cos\omega(t' - t''). \tag{A.0.7}
\end{aligned}$$

Applying the Fourier transform we find

$$
\begin{aligned}
\frac{1}{2}\langle\{F_\alpha(\omega'), F_\alpha(\omega'')\}\rangle =& \frac{\hbar}{\pi} \int_{-\infty}^{\infty} dt' e^{i\omega' t'} \int_{-\infty}^{\infty} dt'' e^{i\omega'' t''} \int_{0}^{\infty} d\omega J_\alpha(\omega) \\
& \cdot \coth\left(\frac{\hbar\omega}{2K_B T}\right) \frac{e^{i\omega(t'-t'')} + e^{-i\omega(t'-t'')}}{2} \\
=& \frac{\hbar}{2\pi} \int_{-\infty}^{\infty} dt' \int_{-\infty}^{\infty} dt'' \int_{0}^{\infty} d\omega J_\alpha(\omega) \\
& \cdot \coth\left(\frac{\hbar\omega}{2K_B T}\right) \left(e^{it'(\omega+\omega')} e^{it''(\omega''-\omega)} + e^{it'(\omega'-\omega)} e^{it''(\omega''+\omega)}\right) \\
=& \; 2\pi\hbar \int_{0}^{\infty} d\omega J_\alpha(\omega) \\
& \cdot \coth\left(\frac{\hbar\omega}{2K_B T}\right) \left[\delta\left(\omega+\omega'\right)\delta(\omega''-\omega) + \delta(\omega'-\omega)\delta(\omega''+\omega)\right] \\
=& \; 2\pi\hbar\delta(\omega'+\omega'') \coth\left(\frac{\hbar\omega'}{2K_B T}\right) \left[J_\alpha(\omega')\Theta(\omega') - J_\alpha(-\omega')\Theta(-\omega')\right].
\end{aligned}
$$
$$(A.0.8)$$

where we have used $\int_{-\infty}^{\infty} dt e^{i\omega t} = 2\pi\delta(\omega)$. Combined with 2.3.6 we find the Fluctuation-Dissipation relation:

$$
\frac{1}{2}\langle\{F(\omega), F(\omega')\}\rangle = 2\pi\hbar\delta(\omega+\omega') \coth\left(\frac{\hbar\omega}{2K_B T}\right) \text{Im}[D_\alpha(\omega)]. \tag{A.0.9}
$$

Appendix B

Integral results

B.1 Laplace transforms

Here are included some Laplace transform results as well as its definition, used previously in the text. The definition used in text is:

$$L[\hat{x}(t)] = \int_0^\infty \hat{x}(t)e^{-st}dt. \tag{B.1.1}$$

Results:

$$L[\ddot{\hat{x}}] = s^2 L[\hat{x}] - s\hat{x}(t_0) - \dot{\hat{x}}(t_0), \tag{B.1.2}$$

$$L^{-1}\left[\frac{s}{s^2 + \omega^2}\right] = \cos\left(\omega(t - t_0)\right), \tag{B.1.3}$$

$$L^{-1}\left[\frac{\omega}{s^2 + \omega^2}\right] = \sin\left(\omega(t - t_0)\right), \tag{B.1.4}$$

$$L^{-1}\left[F(s)G(s)\right] = f(t) * g(t) = \int_{t_0}^t f(t')g(t - t')dt'. \tag{B.1.5}$$

B.2 Fourier transforms

In the same manner, we include different useful Fourier transform results applied previously. The definition of the Fourier transform and its inverse are:

$$F[\hat{x}(t)] = \hat{X}(\omega) = \int_{-\infty}^\infty dt e^{i\omega t}\hat{x}(t), \tag{B.2.1}$$

$$F^{-1}[\hat{X}(\omega)] = \hat{x}(t) = \frac{1}{2\pi}\int_{-\infty}^\infty dt e^{-i\omega t}\hat{X}(\omega). \tag{B.2.2}$$

Some useful results:

$$F[\dot{\hat{x}}] = -i\omega\hat{X}(\omega), \tag{B.2.3}$$

$$F[\ddot{\hat{x}}] = -\omega^2\hat{X}(\omega), \tag{B.2.4}$$

$$F[f(t) * g(t)] = F(\omega)G(\omega). \tag{B.2.5}$$

Appendix C

Details on integration method and numerical calculation difficulties

The integration method employed in this work has been `scipy.integrate.quad` since it has the advantage of integrating with improper limits $(-\infty, \infty)$ by means of a scale scheme. However, the integration method gives some problems due to the slow convergence of some terms of the covariance matrix at low temperatures. A study on the integrands and integration method needs to be taken before continuing with this method forward for large chains. This numerical errors arise even in small chains, we will use the case of a two oscillator model as an example (see figure C.1). It is important to highlight that the results obtained throughout the rest of this work didn't yield any errors, as proper combination of parameters where chosen to avoid this problem.
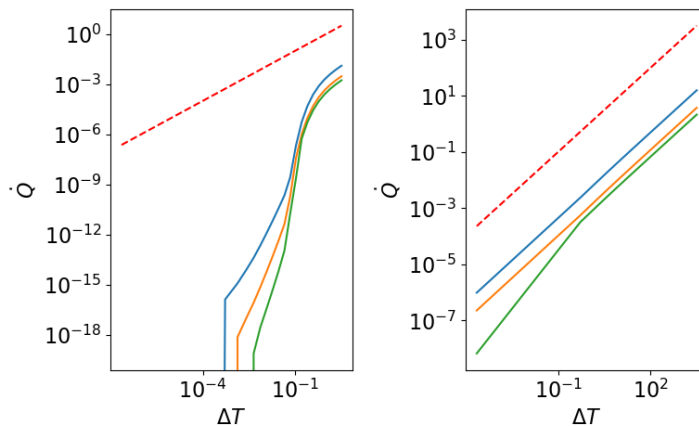

Figure C.1: Evolution of $\dot{Q}$ with ΔT for a two oscillator system with two baths at different temperatures where $\gamma = 10^{-2},\ k = 1$.

While the asymptotic behaviour at high temperature differences is correct, the integrator has problems at low temperatures. This is not an isolated phenomena as can be seen in figure C.2 and the super ohmic spectral density seems more sensitive than the ohmic one. What happened in figure C.1 is attributed to an increase of tolerance in the integrator. This has to do with how `sicpy.integrate.quad` divides the scaled space in order to optimise the integration. Since the features on this domain are too complicated for the division limit imposed initially, it requires a higher tolerance in order to perform the calculation and ignores certain segments in the critical domain of integration, raising an error. Thus, the
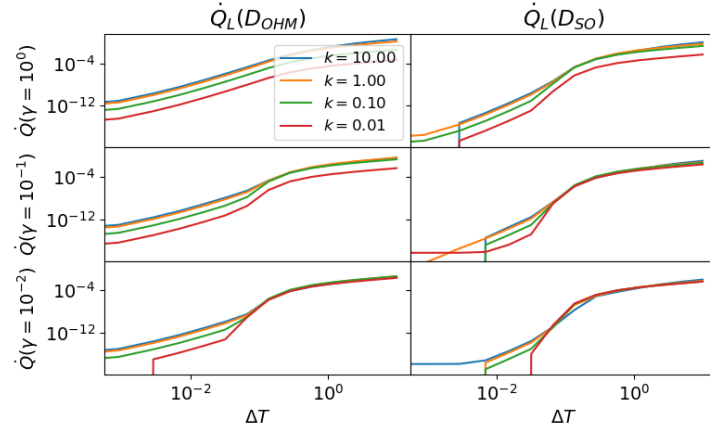
Figure C.2: Evolution of $\dot{Q}_L$ with respect to ΔT of a two oscillator and two bath scheme for different combinations of γ, k and spectral density. For low values of γ the integration method flags an error and computes the values imprecisely in a certain domain. $T_R = 10^{-3}, \Lambda = 10, m_i = 1$.

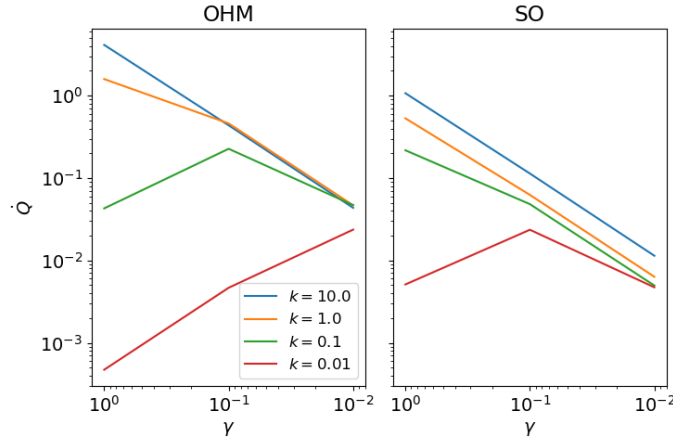integration method shows clearly defective values for certain combinations of γ, k when ΔT is small.

Figure C.3: Evolution of $\dot{Q}_L$ with γ for different values of k with $\Delta T = 10$. Same parameters as in figure C.2

One can also see the values of γ and k compete in defining this shift in figure C.3, which represents the current in figure C.2 at a fixed value of ΔT. This values are in principle unaffected by the numerical error since they are taken at high ΔT. The values seem to converge when γ is small for each model but with larger values the split for different values of k is bigger. Thus, the spectral density is not the only responsible for the difference in heat currents when comparing two spectral densities, the values of γ and k need to be taken into account as well.

The code used on this work can be found on `https://gitlab.com/tanahy/qlangevin`

Bibliography

[1] U. Weiss, *Quantum dissipative systems*. New Jersey: World Scientific, 4th ed ed., 2012.

[2] P. Caldirola, "Forze non conservative nella meccanica quantistica," *Nuovo Cim*, vol. 18, pp. 393–400, Nov. 1941.

[3] E. Kanai, "On the Quantization of the Dissipative Systems," *Progress of Theoretical Physics*, vol. 3, pp. 440–442, Dec. 1948.

[4] H. Dekker, "Quantization of the linearly damped harmonic oscillator," *Phys. Rev. A*, vol. 16, pp. 2126–2134, Nov. 1977.

[5] K. Yasue, "Quantum mechanics of nonconservative systems," *Annals of Physics*, vol. 114, pp. 479–496, Sept. 1978.

[6] S. Nakajima, "On Quantum Theory of Transport Phenomena: Steady Diffusion," *Prog. Theor. Phys.*, vol. 20, pp. 948–959, Dec. 1958.

[7] R. Zwanzig, "Ensemble Method in the Theory of Irreversibility," *The Journal of Chemical Physics*, vol. 33, pp. 1338–1341, Nov. 1960.

[8] I. Prigonine and P. Résibois, "On the kinetics of the approach to equilibrium," *Physica*, vol. 27, pp. 629–646, July 1961.

[9] I. R. Senitzky, "Dissipation in Quantum Mechanics. The Harmonic Oscillator," *Phys. Rev.*, vol. 119, pp. 670–679, July 1960.

[10] H. Mori, "Transport, Collective Motion, and Brownian Motion," *Prog. Theor. Phys.*, vol. 33, pp. 423–455, Mar. 1965.

[11] J. O. González, L. A. Correa, G. Nocerino, J. P. Palao, D. Alonso, and G. Adesso, "Testing the Validity of the 'Local' and 'Global' GKLS Master Equations on an Exactly Solvable Model," *Open Syst. Inf. Dyn.*, vol. 24, p. 1740010, Dec. 2017.

[12] U. Eckern, W. Lehr, A. Menzel-Dorwarth, F. Pelzer, and A. Schmid, "The quasiclassical Langevin equation and its application to the decay of a metastable state and to quantum fluctuations," *J Stat Phys*, vol. 59, pp. 885–934, May 1990.

[13] A. O. Caldeira and A. J. Leggett, "Quantum tunnelling in a dissipative system," *Annals of Physics*, vol. 149, pp. 374–456, Sept. 1983.

[14] A. O. Caldeira and A. J. Leggett, "Path integral approach to quantum Brownian motion," *Physica A: Statistical Mechanics and its Applications*, vol. 121, pp. 587–616, Sept. 1983.

[15] S. Chandrasekhar, "Stochastic Problems in Physics and Astronomy," *Rev. Mod. Phys.*, vol. 15, pp. 1–89, Jan. 1943.

[16] H. Meyer, T. Voigtmann, and T. Schilling, "On the non-stationary generalized Langevin equation," *The Journal of Chemical Physics*, vol. 147, p. 214110, Dec. 2017.

[17] E. B. Saff and A. D. Snider, *Fundamentals of complex analysis for mathematics, science, and engineering.* Englewood Cliffs, N.J: Prentice Hall, 2nd ed ed., 1993.

[18] N. Freitas and J. P. Paz, "Fundamental limits for cooling of linear quantum refrigerators," *Phys. Rev. E*, vol. 95, p. 012146, Jan. 2017.

[19] R. Kubo, ed., *Statistical mechanics: an advanced course with problems and solutions.* North-Holland personal library, Amsterdam: North-Holland, 2. ed., 5. impression (paperback) ed., 1999.

[20] M. Mehboudi, A. Sanpera, and J. M. R. Parrondo, "Fluctuation-dissipation theorem for non-equilibrium quantum systems," *Quantum*, vol. 2, p. 66, May 2018. arXiv: 1705.03968.

[21] A. Shimizu and K. Fujikura, "Quantum Violation of Fluctuation-Dissipation Theorem," *J. Stat. Mech.*, vol. 2017, p. 024004, Feb. 2017. arXiv: 1610.03161.